



CHALMERS
UNIVERSITY OF TECHNOLOGY

Commutation Failure Prevention for HVDC

Improvement in algorithm for commutation failure prevention in
LCC HVDC

Master's Thesis in Electric Power Engineering

INNOCENT OKETCH

Department of Energy and Environment
CHALMERS UNIVERSITY OF TECHNOLOGY
Gothenburg, Sweden 2016

MASTER'S THESIS 2016

Commutation Failure Prevention for HVDC

Improvement in algorithm for commutation failure prevention in
LCC HVDC

INNOCENT OKETCH



CHALMERS
UNIVERSITY OF TECHNOLOGY

Department of Energy and Environment
Division of Electric Power Engineering
CHALMERS UNIVERSITY OF TECHNOLOGY
Gothenburg, Sweden 2016

Commutation Failure Prevention for HVDC
Improvement in algorithm for commutation failure prevention in LCC HVDC
INNOCENT OKETCH

© INNOCENT OKETCH, 2016.

Supervisor: Barry Carolan
PSDC/TST
ABB AB
Ludvika, Sweden

Examiner : Tarik Abdulahovic
Department of Energy and Environment
Chalmers University of Technology
Gothenburg, Sweden

Master's Thesis 2016
Department of Energy and Environment
Division of Electric Power Engineering
Chalmers University of Technology
SE-412 96 Gothenburg
Telephone +46 31 772 1000

Printed by Chalmers Library, Reproservice
Gothenburg, Sweden 2016

Commutation Failure Prevention for HVDC
Improvement in algorithm for commutation failure prevention in LCC HVDC
OKETCH INNOCENT
Department of Energy and Environment
Chalmers University of Technology

Abstract

Line commutated HVDC systems are widely used due to their high power ratings. However, one of the disadvantages of such HVDC systems is the high risk of commutation failures when AC disturbances arise. These failures normally develop in the inverter station. When failed commutation occurs, the LCC HVDC system is greatly disturbed resulting in loss of power transmission. Moreover, the rapid increase in the direct current during unsuccessful commutation results in additional stresses on the thyristor valves.

In an attempt to reduce the probability of unsuccessful commutation, a commutation failure prevention function is added to the HVDC system controls. When an AC system disturbance is detected, this function is activated with the aim of altering the firing order at the inverter station. Since the angle contribution from the function is independent of the minimum inverter extinction angle, this approach possesses limitations under certain AC faults.

In this thesis, a commutation failure prevention function based on voltage-time area contribution was designed and implemented. Simulation results show that both the proposed and existing functions are equally ineffective in mitigating the first commutation failures when three phase faults are applied. However, the proposed function is more effective in mitigating the first commutation failure when single phase faults are applied compared to the existing function. In 17% of the investigated cases, improvements were registered when the proposed function was utilised. Moreover, in 25% of the cases when three phase faults were applied, the proposed function reduced the occurrence of multi-valve commutation failures.

Keywords: LCC HVDC transmission systems, commutation failure prevention, AC faults

Acknowledgements

In view of their invaluable help, I would like to extend my sincere appreciation and gratitude to Magnus Orhstrom for offering me an opportunity to carry out my research at ABB and to my supervisor Barry Carolan for his guidance, patience and thought-provoking discussions throughout the thesis project. To the TST department employees, thank you for all the vital information, ideas and for providing me with a lovely work environment.

Also, I would like to express my heartfelt gratitude to my examiner, Dr. Tarik Abdulahovic for his guidance, support and for tirelessly reviewing my reports.

Special thanks go to the Swedish Institute (SI) for fully funding my study and stay in Sweden, through the prestigious SI study scholarship.

Finally, I would like to thank my family and friends especially my dear wife, Vivian, for their love, patience and encouragement. I dedicated this work to Vivian, Vianney and Maria.

Innocent Oketch, Ludvika, June 2016.

Contents

List of Figures	xi
List of Tables	xiii
1 Introduction	1
1.1 Background	1
1.2 Aim	2
1.3 Thesis Structure	2
2 HVDC Basics	5
2.1 HVDC Technology	5
2.2 HVDC Configurations	7
2.3 Line Commutated Converters	8
2.4 Commutation Process	10
3 HVDC Control	13
3.1 Basic control characteristics	14
3.2 Co-operation between rectifier and inverter	16
3.2.1 Improved voltage-current Characteristic	18
3.3 Converter control system	20
3.3.1 Voltage dependent current order limiter	21
3.3.2 Converter Firing Control	23
4 Commutation Failure	25
4.1 Causes of Commutation Failure	27
4.2 Mitigation of Commutation Failure	28
4.3 Recovery from Commutation Failure	28
5 Commutation Failure Detection and Prevention	31
5.1 Simulation Model	32
5.1.1 AC Network Model	33
5.1.2 AC system disturbances	34
5.2 Existing CFPprev Function	34
5.3 Proposed CFPprev function	39
6 Results and Discussions	41

6.1	AC Faults	43
6.1.1	Strong Network	43
6.1.1.1	Single phase to ground faults	43
6.1.1.2	Three phase to ground faults	51
6.1.2	Weak Network	55
6.1.2.1	Single phase to ground faults	55
6.1.2.2	Three phase to ground faults	59
6.2	Point of wave scan	63
6.2.1	Strong Network	63
6.2.1.1	Single phase to ground faults	63
6.2.1.2	Three phase to ground faults	64
6.2.2	Weak Network	66
6.2.2.1	Single phase to ground faults	66
6.2.2.2	Three phase to ground faults	67
6.3	Comparison of different SCRs	69
7	Conclusions	71
7.1	Future Work	72
	Bibliography	73
A	Appendix 1	I

List of Figures

2.1	HVDC transmission modes (a) Monopolar ground return (b) Monopolar metallic return and (c) Bipolar connection configuration.	7
2.2	The basic three phase six pulse converter	9
2.3	Equivalent circuit for the commutation process	11
2.4	Commutation process and angle relationships	11
3.1	Static voltage-current characteristic of a converter.	15
3.2	Combined static voltage-current characteristic for inverter and rectifier.	17
3.3	Slight AC voltage reduction in the (a) Inverter network (b) Rectifier network.	18
3.4	Improved combined static voltage-current characteristic	19
3.5	The basic converter control system	20
3.6	VDCOL characteristics	22
3.7	Area minimum (AMIN) function	23
3.8	Constant beta function	24
4.1	Valve currents during successful commutation	26
4.2	Valve currents during a failed commutation	26
5.1	The simulation model setup	32
5.2	Commutation failure prediction function (CFPred)	35
5.3	Commutation failure detection function	37
5.4	Commutation failure prevention function	38
5.5	Proposed changes to the CFPprev function	39
6.1	Single phase to ground fault with 84% remaining voltage, existing CFPprev function, Rectifier.	44
6.2	Single phase to ground fault with 84% remaining voltage, existing CFPprev function, Inverter.	45
6.3	Single phase to ground fault with 84% remaining voltage, existing CFPprev function, Inverter.	46
6.4	Single phase to ground fault with 84% remaining voltage, proposed CFPprev function, Rectifier.	48
6.5	Single phase to ground fault with 84% remaining voltage, proposed CFPprev function, Inverter.	49

6.6	Single phase to ground fault with 84% remaining voltage, proposed CFPprev function, Inverter.	50
6.7	Three phase to ground fault with 85% remaining voltage, existing CFPprev function, Inverter.	51
6.8	Three phase to ground fault with 85% remaining voltage, existing CFPprev function, Inverter.	52
6.9	Three phase to ground fault with 85% remaining voltage, proposed CFPprev function, Inverter.	53
6.10	Three phase to ground fault with 85% remaining voltage, proposed CFPprev function, Inverter.	54
6.11	Single phase to ground fault with 87% remaining voltage, existing CFPprev function, Inverter.	55
6.12	Single phase to ground fault with 87% remaining voltage, existing CFPprev function, Inverter.	56
6.13	Single phase to ground fault with 87% remaining voltage, proposed CFPprev function, Inverter.	57
6.14	Single phase to ground fault with 87% remaining voltage, proposed CFPprev function, Inverter.	58
6.15	Three phase to ground fault with 90% remaining voltage, existing CFPprev function, Inverter.	59
6.16	Three phase to ground fault with 90% remaining voltage, existing CFPprev function, Inverter.	60
6.17	Three phase to ground fault with 90% remaining voltage, proposed CFPprev function, Inverter.	61
6.18	Three phase to ground fault with 90% remaining voltage, proposed CFPprev function, Inverter.	62
6.19	Relationship between Amin-ref-gain and SCR	69
A.1	Existing CFPprev function, inverter.	I
A.2	Existing CFPprev function, Inverter.	II
A.3	Proposed CFPprev function, Amin-ref-gain = 0.5, Inverter.	III
A.4	Proposed CFPprev function, Amin-ref-gain = 0.5, Inverter.	IV
A.5	Proposed CFPprev function, Amin-ref-gain = 2, Inverter.	V
A.6	Proposed CFPprev function, Amin-ref-gain = 2, Inverter.	VI

List of Tables

5.1	Simulation model parameter settings.	33
5.2	Impedance values for different SCRs.	33
6.1	Variables presented in the results	42
6.2	Improvements in commutation failure prevention during single phase faults, strong network.	63
6.3	Improvements in commutation failure prevention during three phase faults, strong network.	64
6.4	Improvements in multi-valve commutation failure prevention during three phase faults, strong network.	65
6.5	Improvements in commutation failure prevention during single phase faults, weak network.	66
6.6	Improvements in commutation failure prevention during three phase faults, weak network.	67
6.7	Improvements in multi-valve commutation failure prevention during three phase faults, weak network.	68

1

Introduction

High Voltage Direct Current (HVDC) systems are widely used in long-distance electric power transmission networks. This is attributable to their advantages such as bulk power transmission with lower energy loss, interconnection of asynchronous networks, and the controllability of HVDC systems, which enhance network stability with varying load dynamics [1].

Each HVDC station consists of more than a converter for rectifying or inverting electric current. In order to obtain technically and economically optimum transmission, the voltage is transformed to a suitable level by a transformer. Moreover, there must be filters on the AC side to smoothen the current from the HVDC valves and reactive power compensation on the AC lines. The converter valve consists of a large number of thyristors connected in series to withstand the high voltage levels utilised in HVDC systems.

For successful switching of a thyristor valve, the internal stored charges should be removed such that the valve can establish forward voltage blocking capability [2]. Otherwise, the preceding valve will re-conduct when it is forward biased, consequently interrupting the current commutation process and increasing the chances of a commutation failure.

Commutation failure can be defined as an adverse dynamic event that occurs when a converter valve that is supposed to turn off, continues to conduct without transferring its current to the next valve in the firing sequence. Its occurrence causes temporary interruption of transmitted power and stresses the converter equipment [3]. Furthermore, it can result in significant direct current increase and thus lead to additional heating of converter valves, consequently shortening their lifespan [4].

1.1 Background

System faults on the AC networks connected to a line-commutated HVDC system with thyristor based technology result in voltage disturbances in the form of voltage magnitude reduction and/or phase shift. If the disturbance is severe enough, the power transmission is interrupted by a so called commutation failure. When a

commutation failure occurs, the normal sequence of rectifying and/or inverting is disturbed.

In an HVDC system dynamic performance study, where the control system is optimized for a certain system, one of the tasks is to adjust a function called Commutation Failure prevention (CFPrev). This function detects disturbances in the AC network and feeds into other parts of the control system so that the probability of a commutation failure occurring is reduced. This method has shown good mitigation capabilities for single phase AC faults, as well as for repeated commutation failures resulting from three phase faults.

Currently, the CFPrev function consists of two different parts: The predictor (CF-Pred) that is always active and outputs a signal when the risk of commutation failure is increased and the detector (CFDet) that acts when a commutation failure has already occurred. On detection of AC faults, CFPrev will give an angle contribution to one of the control blocks resulting in earlier firing, consequently increasing the commutation margin and mitigating commutation failure or further commutation failures. CFPrev also sends the angle contribution to another control block to get a reduction in the maximum limit of the firing angle. This is done to allow for earlier firing of the next valve in the firing sequence.

The existing CFPrev outputs an angle contribution which is independent of the minimum extinction angle allowed. This poses a challenge because under certain fault cases, the angle contribution is limited and thus insufficient to mitigate commutation failures.

1.2 Aim

This thesis aims at designing and implementing a new CFPrev function based on a voltage-time area contribution instead of an angle contribution as is the case with the existing function. CFPrev based on angle contribution is largely independent of the extinction angle at which the inverter is operating. Furthermore, this thesis seeks to evaluate the performance improvements of the proposed CFPrev function.

1.3 Thesis Structure

This thesis report comprises seven chapters. The first chapter provides the background and aim of the research. In chapter 2, HVDC basics such as its configurations and technology are discussed. The current commutation process is also presented in this chapter. HVDC control is discussed in chapter 3 while the causes and mitigation of commutation failure are described in chapter 4.

Chapter 5 delves into the commutation failure detection and prevention functions. The methodology of the research and the simulation model utilised in this work are described. The simulation results are presented in chapter 6. The conclusions drawn from the thesis work as well as recommendations for future work are presented in the final chapter.

2

HVDC Basics

In this chapter, important theoretical aspects relating to HVDC basics such as HVDC technology, configurations and Line Commutated Converters (LCC) are discussed.

2.1 HVDC Technology

A typical line commutated converter HVDC system consists of at least one converter station at the sending and receiving ends and the transmission medium. The converter stations at each end are similar and contain converters, converter transformers, harmonic filters, shunt capacitors and DC smoothing reactors.

Converter Station

The main component of the converter station is the converter which consists of thyristor valves. The converter is responsible for power conversion either from AC to DC (rectifier) or DC to AC (inverter) depending on what is desired. Each thyristor valve consists of a certain number of series-connected thyristors so as to attain the required voltage level. The thyristor valves are either arranged into six pulse or twelve pulse groups. The switching of the valves is ordered by the converter control system; all communication between the control and each valve is usually achieved through fibre optics [5].

The converter transformers; steps down the AC voltage of the connected AC system to be supplied to the DC system at the rectifier end [6]. On the inverter end, they step up the AC voltage before it's fed into the receiving AC network. Basically, the transformers adjust the supply's AC voltage level to the required DC voltage level of the HVDC system. These transformers also provide galvanic isolation between the AC and DC systems. The converter transformers largely contribute to the commutation reactance due to their sizeable leakage reactance. Usually, the transformers are of single phase three winding type connected in a wye-wye-delta configuration [5]. A combination of single phase two winding transformers connected in a wye-wye and wye-delta configuration can be used as well. However, the use of three phase transformers is limited by the power requirements, cost, weight and the requirement

of a spare transformer.

The converter operation generates harmonic voltages and currents on both the AC and DC sides. These harmonics contribute to losses and lead to additional heating within the converters. On the AC side of a k -pulse converter, current and voltage harmonics of the $nk \pm 1$ ($n=1,2,3,\dots$) are generated. AC filters are installed to absorb these harmonic components, thus limiting the amount of harmonics and reducing the voltage distortion in the network [5]. High pass filters are used as AC filters [6]. On the DC side of a k -pulse converter, the order of DC harmonics is nk ($n=1,2,3,\dots$). DC filters reduce the harmonics flowing out into the dc line. DC filters are not required in pure cable transmission or back-to-back HVDC schemes. However, it is essential to install them where overhead lines form part of the transmission system to aid in the reduction of telecommunication interference [5].

In steady state operation, line commutated converters consume reactive power during the power conversion process. The shunt capacitors and/or other reactive power sources are installed at the converter AC bus to supply the reactive power required to maintain the converter AC bus voltage. To achieve suitable reactive power compensation, the shunt capacitors are normally subdivided and switched by circuit breakers as the power conversion level varies. Some or all of the shunt capacitors are normally configured as AC harmonic filters [5][6].

The DC reactor contributes to the smoothing of the DC current by reducing the direct current ripples, thus reducing the harmonic voltage in the DC line and preventing the extinction of the direct current at low power levels. The smoothing reactors also protect the converter valves by limiting the fast rise of current flowing through the converter during commutation failures [6]. Moreover, they enable the limitation of the crest current during a short-circuit fault on the DC line. It should be noted that the inductance of the converter transformer also contributes significantly to these functions.

Transmission medium

Cables, overhead lines or a combination of the two form the transmission medium between two or more converter stations. The cables are either underground or undersea depending on the particular DC link route. Electrode connections are utilised for back-to-back systems. Most of existing HVDC systems use the ground return in normal operating conditions (monopolar systems) or in emergency conditions (bipolar systems). However, due to environmental and safety concerns, the utilisation of ground return is becoming increasingly discouraged and the use of the more expensive metallic return is greatly encouraged, in particular for monopolar systems.

2.2 HVDC Configurations

HVDC transmission systems can be configured in many ways to suit operational requirements. They are either point to point systems or HVDC multi-terminal systems. Point to point HVDC systems are either monopolar or bipolar.

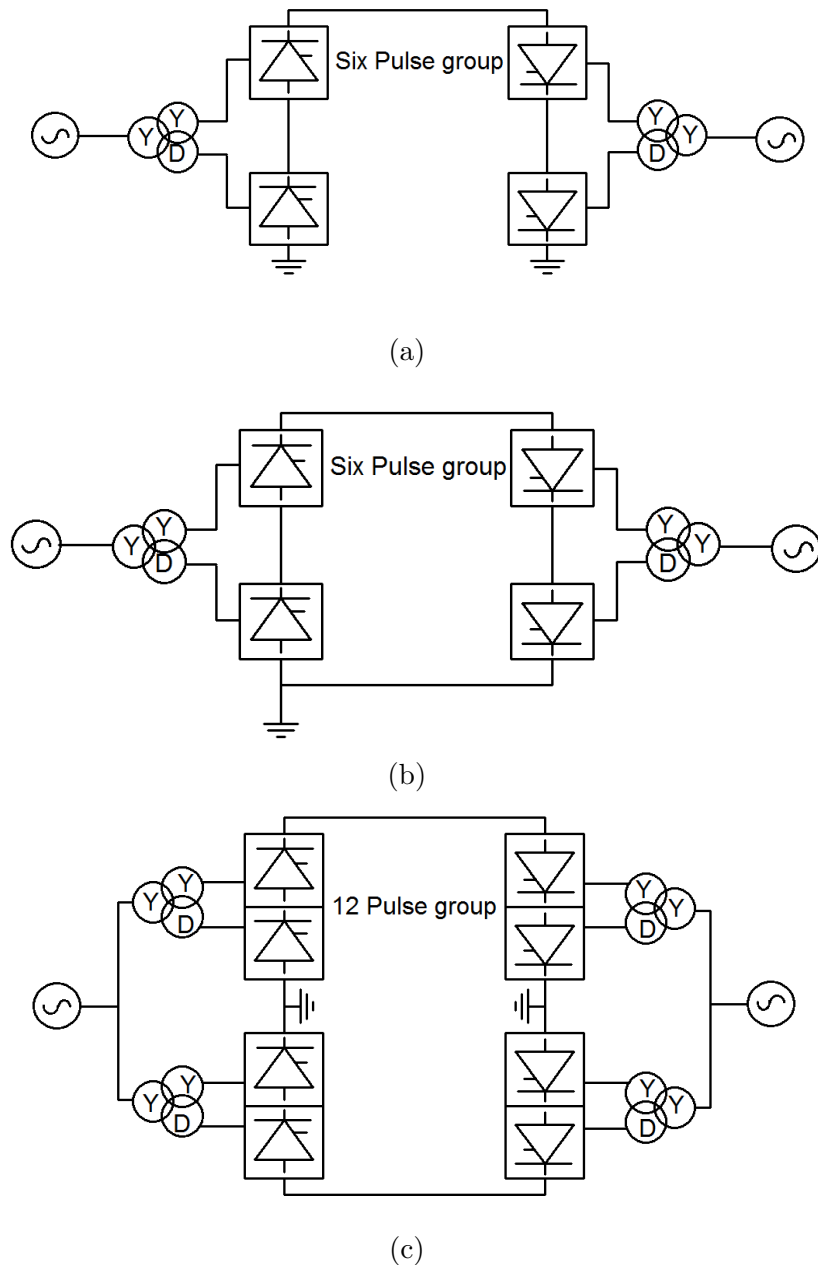


Figure 2.1: HVDC transmission modes (a) Monopolar ground return (b) Monopolar metallic return and (c) Bipolar connection configuration.

Monopolar HVDC systems

Monopolar systems consist of one pole at each converter station and utilise a single high voltage conductor and a return path. The return path is either through the ground/sea or a dedicated metallic return conductor as shown in Fig. 2.1a and 2.1b respectively. This configuration is widely used when the power is transferred through underground or undersea cables. However, the cable installation costs largely influence the decision. Where the ground resistance is too high, monopolar systems with metallic return path are preferred to those with earth return [6]. Moreover, in recent schemes, the use of earth return is becoming less common because of environmental concerns associated with it.

Bipolar HVDC systems

Bipolar systems consist of two series-connected poles at each converter station, one of positive polarity and the other negative polarity, with their neutral points grounded. This is the most preferred configuration because of its large power transfer capability compared to the monopolar system. Fig. 2.1c shows a simplified single-line diagram of a two-terminal bipolar HVDC transmission system. During steady state operation, the same current flows through each pole, hence no current flows through the ground. When one of the poles in a converter station malfunctions or is out of service, the other pole can still transmit power with the ground as the return. Reverse power flow can be achieved and controlled by altering the polarities of the two poles at both converter stations [6].

Back to Back systems

In back-to-back systems, both the rectifier and inverter are located at the same site. This is the simplest configuration and a special case of HVDC transmission systems where no DC transmission link is required [7]. In general, back-to-back systems are used to interconnect two asynchronous AC systems.

Multi-terminal systems

These are HVDC systems that consist of three or more converter stations; at least one rectifier and one inverter station is required. Its architecture, communication network between the converter stations and control systems are more complex in comparison to the point to point systems [6].

2.3 Line Commutated Converters

Various HVDC schemes employ line commutated thyristor valve converters. In a line commutated converter, the process of current commutation is facilitated by the connected AC system voltage. The Graetz bridge is the basic unit for HVDC line commutated converters. It consists of six thyristors assembled in form of three phase

legs. Each phase leg contains two thyristors, the center points are connected to a three phase power supply. This three phase full-wave bridge circuit is shown in Fig. 2.2.

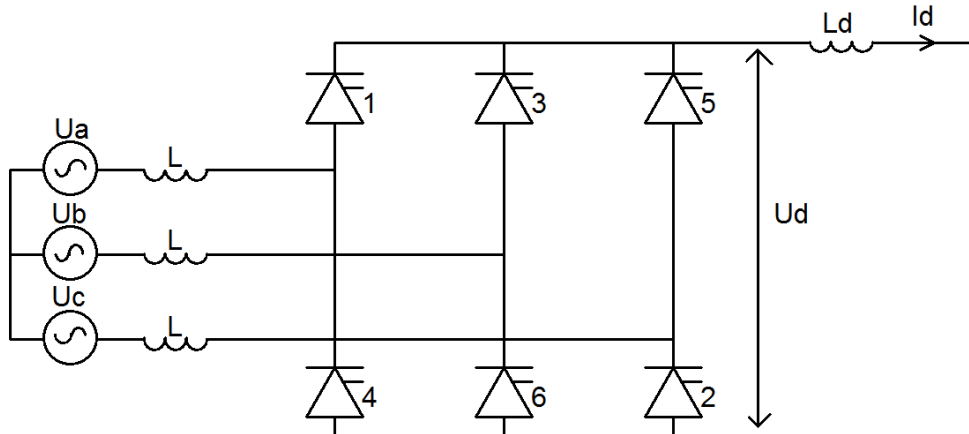


Figure 2.2: The basic three phase six pulse converter

In Fig. 2.2. 1 to 6 are the thyristor valves, L is the total commutation inductance per phase seen by the valves, $U_{a,b,c}$ are the source voltages of the AC network, U_d and I_d are the DC voltage and direct current respectively. L_d is a large DC inductance to ensure that the ripples in the direct current are significantly reduced.

Consider that valve 1 is fired during an interval when it is forward biased (its anode voltage is positive with respect to the cathode) such that it is conducting current. An alternating line voltage U_{ba} appears across valve 3. When U_{ba} is in its negative cycle, valve 3 experiences a negative voltage across it (reverse biased) and cannot conduct current even when a firing pulse is provided. Once the line voltage switches to its positive cycle, valve 3 is forward biased. If valve 3 is fired during this interval, it will conduct current and consequently, valve 1 experiences a negative voltage across its terminals.

Through the consecutive firing of incoming thyristor valves while the line voltage across their terminals are of appropriate polarity, each thyristor can be successfully commutated. The incoming thyristor valves causes the application of a line voltage to the outgoing valve which reverse biases the outgoing valve. The term line commutated converter arises because an alternating line voltage is required to serve as the commutating voltage, and should have a polarity that will reverse bias the outgoing thyristor valve.

The thyristor valves do not turn on at the point in the AC cycle at which they become forward biased. Subsequent to being forward biased, a thyristor valve must receive a firing pulse before it starts to conduct. The duration between receiving the forward voltage and start of conduction is usually expressed in angular measure and is referred to as firing or delay angle.

Theoretically, the delay angle ranges from 0° to 180° . When the delay angle lies between 0° to 90° , the converter is said to be operating in the rectifier mode. On the other hand, when the delay angle lies between 90° to 180° , the converter is said to be operating in inverter mode. However, in practice, the minimum delay angle is about 5° for rectifier operation and the inverter operation range is from 110° to 165° . The adjustable delay angle enables the control of the converter's voltage conversion ratio.

In rectifier mode, the direct current flows from the positive polarity of the DC circuit, this facilitates conversion from AC to DC. Conversely, in inverter mode, the direct current flows from the negative polarity of the DC circuit therefore facilitating conversion from DC to AC [2]. An HVDC system basically consists of two twelve pulse groups with each group comprising two Graetz bridges. One group operates in rectifier mode with the other operating in inverter mode.

2.4 Commutation Process

The switching of current conduction from one of the thyristor valves to another in the same row of a converter bridge is referred to as commutation. Fig. 2.2 showing a basic six pulse converter is utilised to describe the commutation process. The direct current, I_d is assumed to be constant during the commutation interval.

Since the current through an inductance cannot change instantaneously, the commutation process takes a certain time. The inductance is due to the reactive converter transformer and the AC grid reactance. This duration of commutation is referred to as overlap time or angle of overlap, it is measured in degrees or radians and denoted by μ [8]. In order to change a current through an inductor, a voltage needs to be applied over the inductor.

Consider a case when valves 1 and 2 are conducting and the direct current is to be commutated from valve 1 to valve 3 in the top row of Fig. 2.2. The commutation can take place as long as the voltage difference $U_b - U_a$ is positive, this voltage difference is referred to as commutating voltage. The commutating voltage is the voltage, which at constant direct current would have occurred across the thyristor valve, if the valve had not been fired [8]. The commutating voltage can also be described as the reverse voltage across the thyristor terminals that serves to turn off the thyristor. During the commutation process, the converter bridge can be represented with an equivalent circuit shown in Fig. 2.3. Valves 1 and 3 are both conducting in the top row while valve 2 in the bottom row continues to conduct as before.

The commutating voltage drives a commutating current i through valve 1 and 3, this commutation current will increase thereby increasing the current flowing through valve 3 while decreasing the current through valve 1.

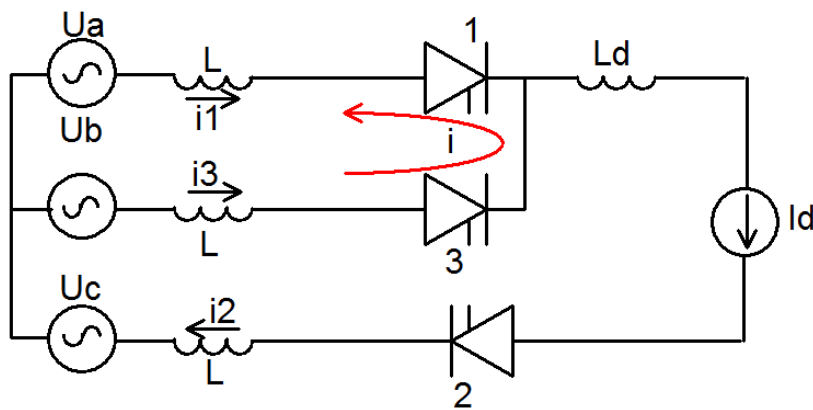


Figure 2.3: Equivalent circuit for the commutation process

The commutation process is complete when the commutation current has increased and is equal to the direct current I_d . This is illustrated in Fig. 2.4, where U_{ba} is the commutation voltage, i is the commutation current, i_1 and i_3 are the currents flowing through valve 1 and valve 3 respectively and area A is the inverter commutation margin.

In the rectifier, valve 3 is fired at α_1 and the commutation of current from valve 1 to valve 3 takes μ_1 . The remaining area, γ_1 , is more than sufficient for successful commutation therefore commutation failures rarely occur in the rectifier. In the inverter, valve 3 is fired at α and the commutation of current from valve 1 to valve 3 takes μ . The remaining voltage-time area A (commutation area) can be greatly reduced in the event of disturbances in the AC network.

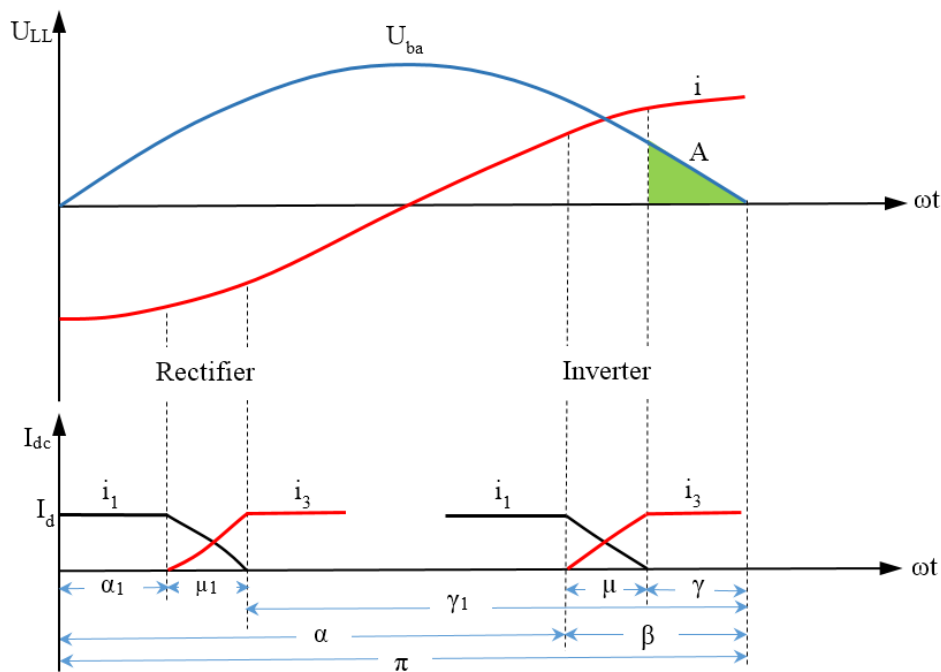


Figure 2.4: Commutation process and angle relationships

Fig. 2.4. shows the delay angle (α), which corresponds to the time when valve 3 is fired after the commutation voltage has turned positive. Mu (μ) is the overlap angle, the angle corresponding to the time when both valves 1 and 3 are conducting. Gamma (γ) is extinction angle or commutation margin, the angle corresponding to the time between when valve 1 is extinguished and when the commutation voltage goes through its zero crossing. During steady state operation, the relationship between these angles is expressed as follows:

$$\alpha + \mu + \gamma = 180^\circ \quad (2.1)$$

A reverse voltage needs to be applied across a thyristor valve for a certain duration. This is required to remove the charges stored during the conduction process such that the valve can withstand a voltage in the forward direction [9]. This negative voltage is applied during the time corresponding to γ , the commutation margin. Moreover, the extinction angle also provides an additional margin to ensure successful commutation when small disturbances occur during normal operation [9].

Considering inverter operation, the expressions for the commutating current and the overlap angle can be derived. The commutating voltage is given by either (2.2) or (2.3).

$$U_{ab} = \sqrt{2} U_{LL} \sin(\omega t) \quad (2.2)$$

$$U_{ab} = 2\omega L \frac{di_\mu}{d(\omega t)} \quad (2.3)$$

Substituting (2.2) into (2.3), rearranging and then integrating during the commutation or overlap duration as shown in (2.4) results in the commutating current, i , expression and is given in (2.5).

$$\int_{\alpha}^{\alpha+\mu} \sqrt{2} U_{LL} \sin(\omega t) d(\omega t) = \int_0^i 2\omega L di_\mu \quad (2.4)$$

$$i = \frac{\sqrt{2} U_{LL}}{2\omega L} [\cos(\alpha) - \cos(\alpha + \mu)] \quad (2.5)$$

The shape of the commutating current (see Fig. 2.4), which gives the time it takes for the current in the succeeding valve to increase is obtained from (2.5) where $\alpha + \mu$ is replaced by ωt . From (2.5), it is clear that the overlap angle depends on the direct current, the AC voltage, the converter transformer inductance, the firing angle and the AC system frequency.

3

HVDC Control

The possibility of setting the DC voltage across the converter valve by varying the firing angle forms the basic control concept of an HVDC transmission system. In order for the inverter valves to conduct, the rectifier must set up a higher voltage than the inverter. The power delivered to the DC circuit from the rectifier is given by (3.1) where P_{d1} is the power, I_d the direct current and U_{d1} is the DC voltage across the rectifier.

$$P_{d1} = U_{d1} \times I_d \quad (3.1)$$

The direct current is dependent on the voltage difference between the rectifier and inverter and the DC line resistance R_d . It is given by (3.2) where U_{d2} is the DC voltage across the inverter.

$$I_d = \frac{(U_{d1} - U_{d2})}{R_d} \quad (3.2)$$

Since the DC line resistance is usually relatively small, (3.2) indicates that the direct current is very sensitive to converter voltage variations. A change in the DC voltage in either converter station leads to large variations in the direct current and therefore large variations in the DC power [10].

By establishing a direct current feedback loop in one of the converter stations, usually the rectifier, while making the other station (inverter) control the DC voltage, a basic HVDC control system is obtained. Through the current feedback loop in the rectifier, the DC voltage difference ($U_{d1} - U_{d2}$) is automatically kept at such a level that a preset direct current can be delivered to the inverter. The current control can be performed by any of the converter stations. However, it should be noted that the current is always controlled by one converter while the voltage is determined by the other [11].

3.1 Basic control characteristics

The relationship between the direct current and direct voltage across the converter is very pivotal in understanding how the two converter stations co-operate to control the power flow on the DC line [12]. The rectifier voltage-current characteristic is given by (3.3) while the inverter voltage-current characteristic is given by (3.5).

$$U_d = U_{dio} \cos \alpha - (d_{xN} + d_{rN}) \frac{U_{dioN}}{I_{dN}} I_d \quad (3.3)$$

where U_d is the average direct voltage, U_{dio} is the ideal no-load direct voltage, U_{dioN} is the nominal no-load direct voltage, α is the rectifier firing/delay angle, I_d is the average direct current, I_{dN} is the nominal direct current, d_{xN} and d_{rN} are the nominal reactive and resistive direct voltage drop in per unit referred to U_{dioN} respectively.

As can be seen from (3.3), three variables, U_{dio} , α and I_d determine the level of the direct voltage U_d across the converter. U_{dio} is proportional to the AC bus voltage and for this discussion, this voltage is assumed to be constant. The term $(d_{xN} + d_{rN}) \frac{U_{dioN}}{I_{dN}}$ is constant and directly proportional to the converter transformer impedance.

$$d_{xN} \frac{I_d}{I_{dN}} = \frac{1}{2} \frac{U_{dio}}{U_{dioN}} [\cos \alpha - \cos(\alpha + \mu)] \quad (3.4)$$

By variable substitution and making use of (2.1) and (3.4), (3.3) can be converted to (3.5) which gives a form suitable for the representation of the inverter voltage-current characteristic.

$$U_d = - [U_{dio} \cos \gamma - (d_{xN} - d_{rN}) \frac{U_{dioN}}{I_{dN}} I_d] \quad (3.5)$$

where γ is the inverter extinction angle. The negative sign on the right hand side of (3.5) means that the inverter region appears in the fourth quadrant of the voltage-current characteristic if the rectifier region is in the first quadrant as can be seen in Fig. 3.1.

The red curve in Fig. 3.1, shows the rectifier static voltage-current characteristic. The maximum value of U_d is achieved when α is at its minimum value and no current is flowing through the DC line (I_d is zero).

Operating with a constant minimum α gives a voltage-current characteristic which starts at point a where $U_d = U_{dio} \cos \alpha_{min}$, and is represented by a negative slope line $a - b$ for increasing I_d . The slope of the line $a - b$ is determined by the rectifier transformer. As the current through the DC line increases to its preset value/current order, we move along the section $a - b$ of the characteristic.

Reaching point b signifies that the direct current is now equal to the preset value. The vertical line in the characteristic represents operating with a constant I_d and

variable α . This is the normal operation mode of the rectifier, where it controls the direct current by changing α to cope with the voltage requirements on the DC side [12]. The position of the vertical line $b - c - d$ is determined by the current order.

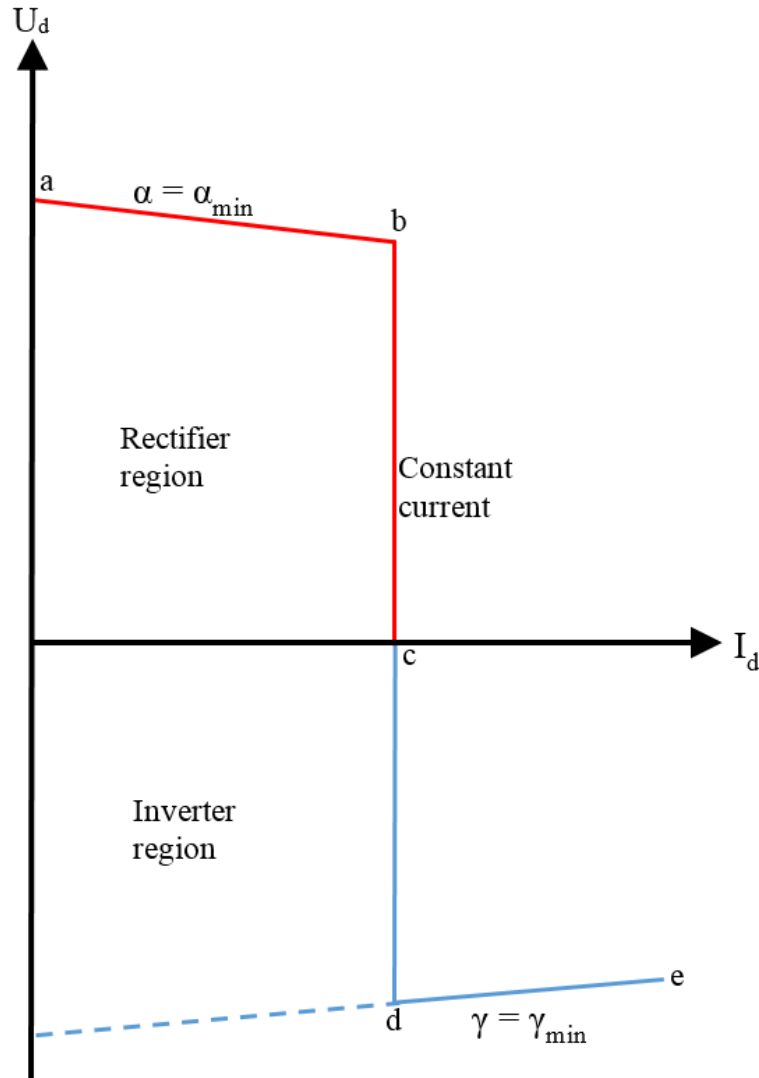


Figure 3.1: Static voltage-current characteristic of a converter.

As α is increased from α_{min} , we move along the section $b - c$, the DC voltage also decreases because of its relation to α . At point c when U_d is zero, α is around 90 degrees and no power is transmitted.

Further increase of α beyond 90 degrees moves the converter from the rectifier region into the inverter region. The inverter characteristic is represented by the blue curve in Fig. 3.1.

Section $c - d$ represents operation with a constant current but with α varying from around 90 degrees (point c) to α_{max} (point d). At point d , α reaches the maximum

permitted value, α_{max} . This α_{max} value is determined by the minimum allowed extinction angle, γ_{min} , and the existing overlap angle, μ .

When the current through the converter is increased, α must decrease and as a result the overlap angle must increase so as to keep U_d constant (see (3.3)). Increasing the direct current means moving along line $d - e$ of the voltage-current characteristic, where the extinction angle is kept constant at γ_{min} . The characteristic $a - b - c - d - e$ is the basic form of the voltage-current characteristics for an HVDC converter for both rectifier and inverter operation.

3.2 Co-operation between rectifier and inverter

In an HVDC transmission system, all converters are equipped with a basic feedback loop current controller. Therefore, any of the converters can control the direct current flowing in the system [10]. The general criteria for the converter to operate either as rectifier or inverter is, that the converter with the highest direct current order will operate as rectifier and the other will operate as an inverter [11].

It should be noted that the sign of the voltage of the characteristics shown in Fig. 3.1 is defined such that the voltage is positive when the cathode side of the valve bridge is positive. However, when discussing co-operation between the rectifier and the inverter, the DC voltage sign definition refers to the DC line. The DC line voltage is positive when the rectifier voltage is positive. Therefore, when the second converter is in inverter mode, its DC voltage will also be positive and its characteristic will be in the first quadrant [12]. In reverse power operation, the DC voltage will become negative in both converters.

Since it is possible to operate both the converters as rectifier or inverter, it is desired to have their combined voltage-current characteristics in the same diagram and quadrant. If the current order in the inverter, I_{OI} , is set a lower than that of the rectifier, I_{OR} , and $U_{dio} \cos \gamma_{min}$ in the inverter is slightly lower than $U_{dio} \cos \alpha_{min}$ in the rectifier, then a combined characteristic for both converters is obtained. This combined characteristic is shown in Fig. 3.2 where the blue curve is the inverter characteristic while the red curve is the rectifier characteristic.

As shown in Fig. 3.2, the unique operation point A is obtained at the intersection of the rectifier and inverter characteristics. At point A, the rectifier controls the current while the inverter determines the voltage through constant extinction angle, γ , control. This is preferred because it results in the lowest reactive power consumption at the inverter [13].

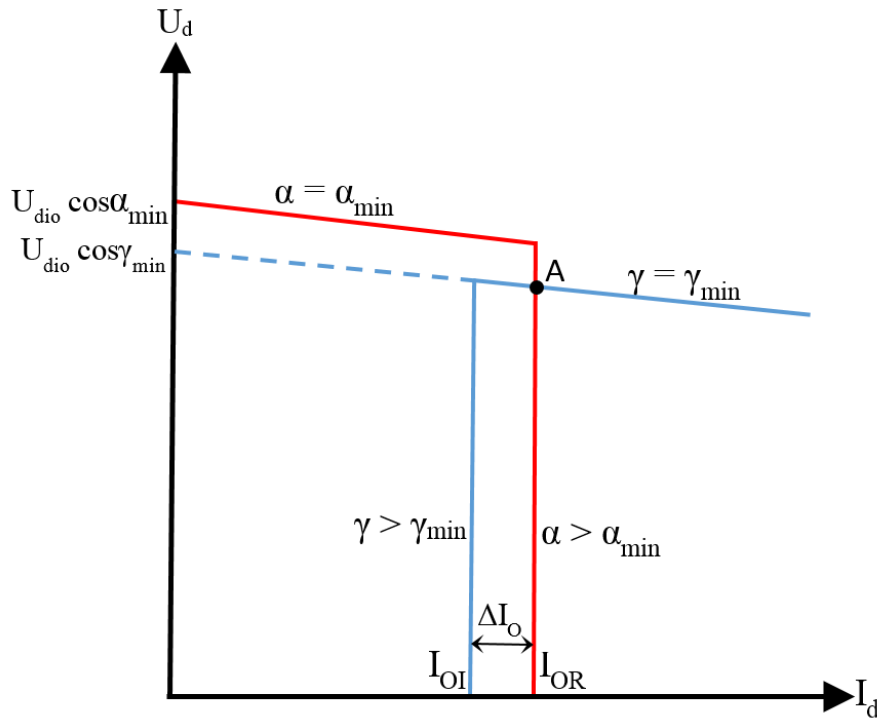


Figure 3.2: Combined static voltage-current characteristic for inverter and rectifier.

The difference between rectifier and inverter current orders, normally around 10% of the nominal current, is referred to as the current margin and is denoted by ΔI_O in Fig. 3.2 [12]. The current margin is required to ensure that the rectifier is controlling the current while the inverter controls the voltage. In practice, both the rectifier and inverter are given equal current orders, but the current margin is subtracted in the inverter current control system. Therefore, the effective inverter current order is lower than that in the rectifier.

Given that the feedback loop current controller seeks to establish the ordered current, the controller in the inverter will increase the inverter firing angle, α , so as to lower the direct current on the DC line (see (3.5)). As the inverter increases α , its extinction angle, γ , reduces. The inverter will increase α until it reaches to its maximum allowed value (minimum γ). At this point, the inverter will output its maximum DC voltage and the HVDC system will be operating at point A as shown in Fig. 3.2.

In the event that the voltage in the inverter AC grid is reduced, the $U_{dio} \cos \gamma_{min}$ and consequently, the inverter DC voltage are reduced as shown by the dotted blue line in Fig. 3.3a, with a new minimum extinction angle, γ' . In order to counter this event, the rectifier, which is controlling the current, will react by increasing its firing angle, α , so as to maintain the direct current at the desired level. Therefore, the operating point will shift from point A to point B as the rectifier's firing angle is increased as illustrated in Fig. 3.3a.

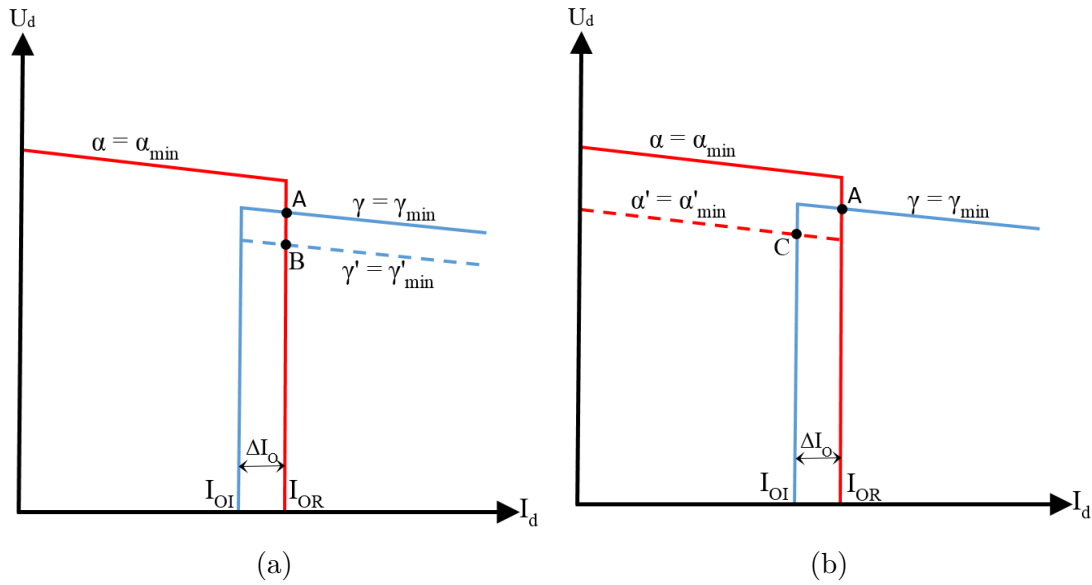


Figure 3.3: Slight AC voltage reduction in the (a) Inverter network (b) Rectifier network.

However, If a voltage reduction occurs in the rectifier AC grid, the rectifier DC voltage drops as shown by the dotted red line in Fig. 3.3b, with a new minimum firing angle, α' . The rectifier direct current will also decrease, the inverter will respond to the decrease in direct current by increasing γ , so as to reduce the inverter DC voltage. The inverter control system will increase γ until the direct current is equal to the inverter current order, I_{OI} . Therefore, the inverter takes over the current control and the operation point shifts from point A to point C as shown in Fig. 3.3b.

3.2.1 Improved voltage-current Characteristic

The DC voltage from an inverter is given by (3.6). From this equation it can be seen that when the inverter is operating with a constant extinction angle, γ , the DC voltage, U_d , will decrease proportionally as the direct current, I_d , is increased. This means that the inverter acts as a negative resistance when operating at constant extinction angle.

$$U_d = U_{dio} \cos \gamma - (d_{xN} - d_{rN}) \frac{U_{dioN}}{I_{dN}} I_d \quad (3.6)$$

This negative resistance creates an undesired situation for the feedback current loop and can result into stability issues especially when the inverter AC network has a high impedance. Therefore, the weaker the AC network is, the more unstable the system will be [10].

An improvement to the combined static voltage-current characteristic for the con-

verters shown in Fig. 3.2 is represented in Fig. 3.4. This modification of the inverter voltage-current characteristic is often applied in HVDC systems to improve the stability of the feedback loop current controller. This improvement, usually referred to as the positive slope, is represented in Fig. 3.4 as the section between a and b .

The positive slope mitigates the stability issues arising from the inverter acting as a negative resistance since it enables operation at a new point D . Along the section a - b , the inverter operates with a constant β where it's expressed as $\beta = \gamma + \mu$. Therefore, the rectifier current order can be increased without causing the inverter DC voltage to decrease. At point b , the end of the positive slope, the inverter then moves to constant extinction angle operation.

Moreover, the positive slope was originally introduced in HVDC control systems to ensure that the nearly parallel characteristics of the rectifier, α_{min} , and inverter, γ_{min} , do not coincide when there is an unfavourable combination of rectifier and inverter AC voltages.

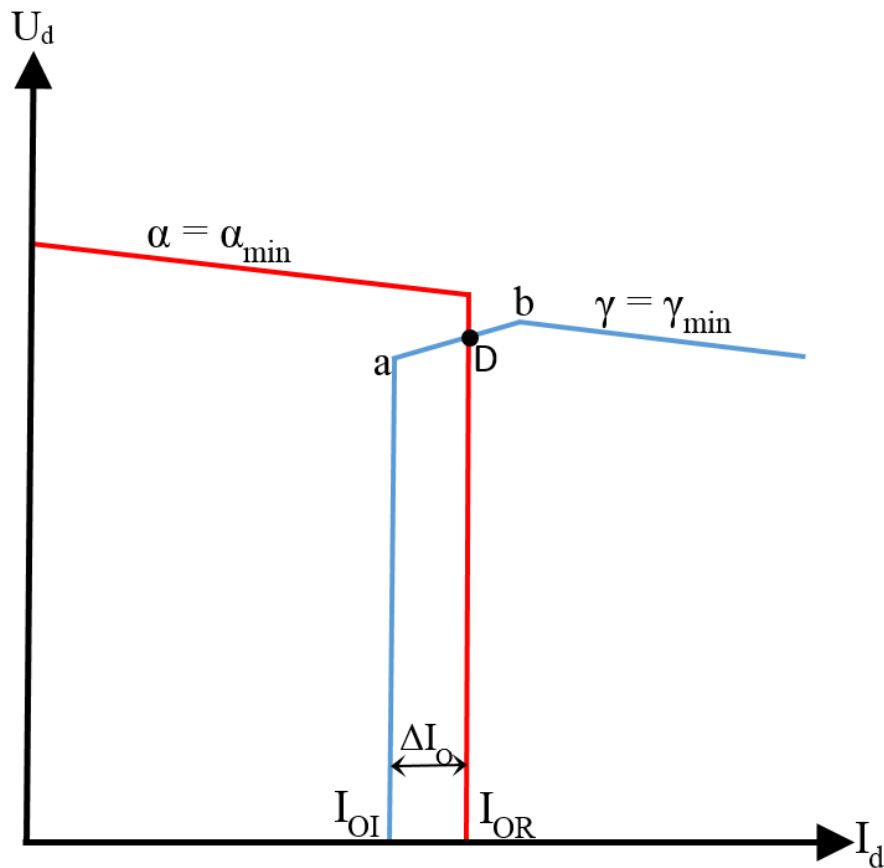


Figure 3.4: Improved combined static voltage-current characteristic

3.3 Converter control system

In this section the basic converter control system required to operate an HVDC transmission is described. The converter control systems are designed and tuned to ensure that the following requirements are achieved[14] [15]:

- No steady state error in the ordered current.
- Fast response of the control system to any AC or DC system disturbance.
- Fast reduction of over voltages and short circuit currents across and through the converter valves respectively.
- Stable system operation whenever transients occur on either the AC networks or the DC link.
- Minimise the occurrence of standing commutation failures during faults and ensure prompt restart of the HVDC system without the development of commutation failure.
- Operation with minimum reactive power consumption.

A block diagram showing the basic converter control system is shown in Fig. 3.5. The functions shown in the block diagram are essentially the same for both the rectifier and the inverter. To differentiate between the rectifier and the inverter operation, both stations are given equal current orders, but the current margin, ΔI_o , is subtracted in the inverter to make the effective current order in that station lower than in the rectifier as can be seen in Fig. 3.4 [11].

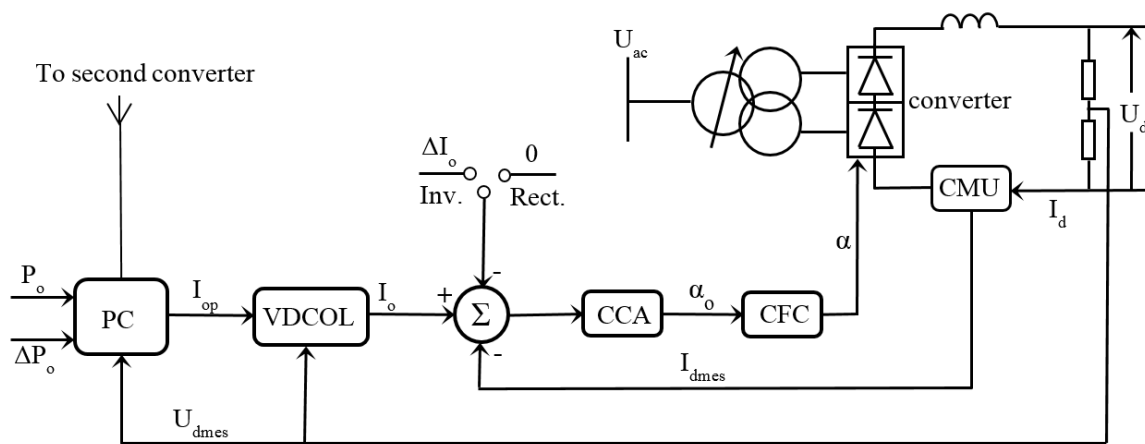


Figure 3.5: The basic converter control system

The system is primarily made up of a feedback (closed) loop direct current controller and an outer open loop direct current controller. The closed loop controller comprises of the Current Control Amplifier (CCA) and the Converter Firing Control unit (CFC), which generates the valve control pulses. The CFC also contains functions used to determine the maximum and minimum firing angle limits. The outside loop consists of the Voltage Dependent Current Order Limiter (VDCOL).

Both the converter stations have master control units. However, only one master control unit is activated while the other remains inactive during normal operation of the transmission system [12]. The station with the active master control is referred to as the lead station while the other is referred to as the trail station.

A power order, P_o , is received by the power control unit (PC) from the HVDC master control. The power order can be received from either of the two converter stations or from a dispatch control center. If the power order is set in one of the stations, this station is referred as the master station and the other is thus a slave station. The additional power order, ΔP_o , if required for power modulation, may be generated in either of the two converter stations [12].

The power control unit then utilises the power order and the measured DC voltage, U_{dmes} , to generate a current order, I_{op} . This current order is then sent to the VDCOL. This unit reduces the current order as the DC voltage decreases to maintain stability during transient disturbances. The generated current order is also sent to the other converter station via a communication link.

The VDCOL unit gives out a voltage dependent current order, I_o , which is then compared with the measured direct current, I_{dmes} , from the current measurement unit (CMU). The obtained current error is sent to the current control amplifier. The CCA then outputs an ordered firing angle, α_o , depending on the magnitude of the current error. The α_o from the CCA then forms the input to the CFC which generates firing pulses for the converter valves.

The internal phase controlled oscillator of the CFC compares the new α_o with the existing firing angle and makes necessary adjustments to the firing angle. Therefore, the current order error will be greatly reduced and possibly zero during steady state operating conditions. Consequently, a closed loop current control is formed [10].

3.3.1 Voltage dependent current order limiter

The purpose of the voltage dependent current order limiter is to prevent power instabilities during and after disturbances in the AC network. In addition, it's used to achieve fast and controlled recovery while suppressing the probability of consecutive commutation failures after the clearance of the AC or DC disturbance [6][10]. To aid the AC system in recovering from faults, the reactive power consumed by the converters should be limited. The VDCOL makes this possible by reducing the transmitted direct current when operating DC voltage is reduced [11].

The VDCOL characteristic is shown in Fig. 3.6. A minimum limit of the current order, I_{omin} is required to prevent converter operation with a current so low that the valves extinguish it during their conduction interval. Usually, I_{omin} is set at 10% of the rated current. The characteristic also includes a maximum limit, I_{omax} , which is normally set at the expected current order.

During normal operation, the DC voltage, U_d , is higher than the voltage, U_{dhigh} , which is the voltage at the break point A. U_{dhigh} is normally set at 70% of the rated voltage [11]. Suppose that U_d drops below U_{dhigh} , the maximum limit of the current order will start to decrease along the section A-B. This will reduce the output current order, I_o , from the VDCOL if the input exceeds the maximum current order limit.

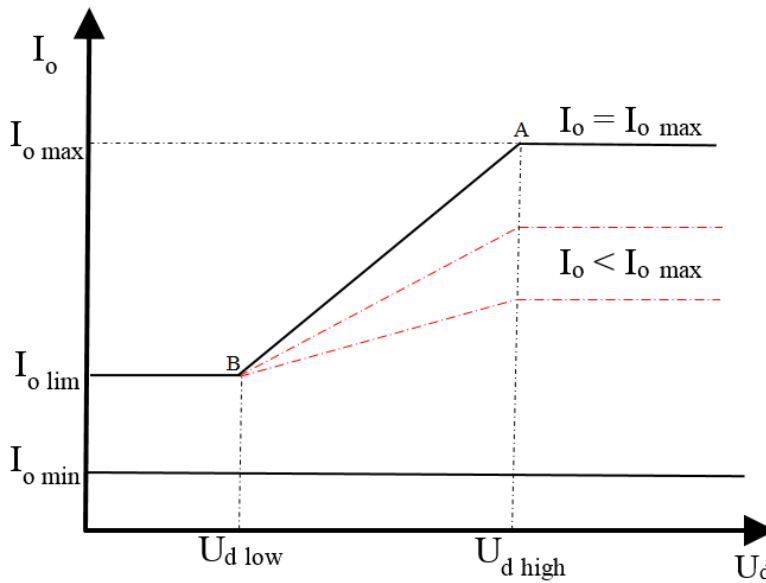


Figure 3.6: VDCOL characteristics

If the direct voltage continues to decrease and point B (where U_d is equal to U_{dlow}) is reached, the reduction of the current order maximum limit stops and the maximum current order limit is held at I_{olim} . I_{olim} is usually set at 30% of the rated current [10].

When the actual current order is below the maximum limit of the current order (somewhere along section A-B), the reduction of the current order will start at a value of U_d that is lower than U_{dhigh} , depending on when the maximum current order limit reaches the actual current order. Such a scenario may result in voltage instability when the inverter AC network is very weak. In order to mitigate this, the VDCOL is designed with the capability to keep U_{dhigh} at the same level for all current orders between I_{omax} and I_{olim} as shown by the dotted red line in Fig. 3.6. In this case, the slope of the maximum current order between the U_{dlow} and the U_{dhigh} will be reduced for current orders lower than the I_{omax} .

3.3.2 Converter Firing Control

The converter firing control block consists of various functions. However, only the Area Minimum and Constant Beta functions (that are essential for this thesis) are briefly described in this section.

Area Minimum (AMIN)

Within the AMIN function, the present commutation area, $Rem - Area$, is calculated and compared with to a minimum allowed reference level, $Amin - ref - final$. Fig. 3.7 shows a simplified block diagram of this function.

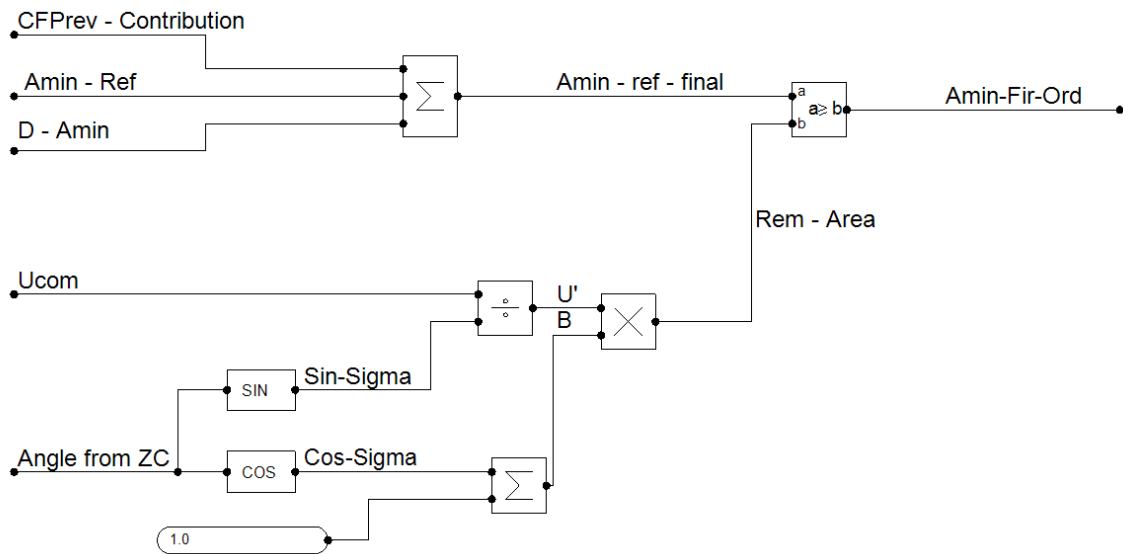


Figure 3.7: Area minimum (AMIN) function

The angle from the previous zero crossing of the commutating voltage, $Angle from ZC$, as well as the commutating voltage magnitude at the firing instant, $Ucom$, are utilised to predict the remaining commutation area, $Rem - Area$. If $Rem - Area$ is below the minimum allowed reference level, a firing signal, $Amin - Fir - Ord$, is sent to the valves. This is done to prevent the occurrence of commutation failures.

The Dynamic Area minimum, $D - Amin$, signal is used to compensate for a transient decrease of the direct current by increasing the $Amin - ref - final$. It also increases the $Amin - ref - final$ where a fast increasing current response is required within the HVDC system. This is necessary to ensure sufficient commutation area during small disturbances in the inverter AC network [10]. When the $D - Amin$ value is non-zero, it is added to the preset $Amin - ref$ value to increase the $Amin - ref - final$.

When AC faults are detected, the CFPprev-Contribution, which is an output from the CFPprev function described in section 5.2, is added to the preset $Amin - Ref$ value to increase the $Amin - ref - final$. This is done to prevent commutation failures.

In the event that a commutation failure has already occurred, the commutation area for the next valve in the firing sequence is increased to avoid further commutation failures.

Constant Beta

The constant beta function is primarily used to realise the improved voltage-current characteristic discussed in section 3.2.1. Fig. 3.8 is of a block diagram showing part of the Constant Beta function.

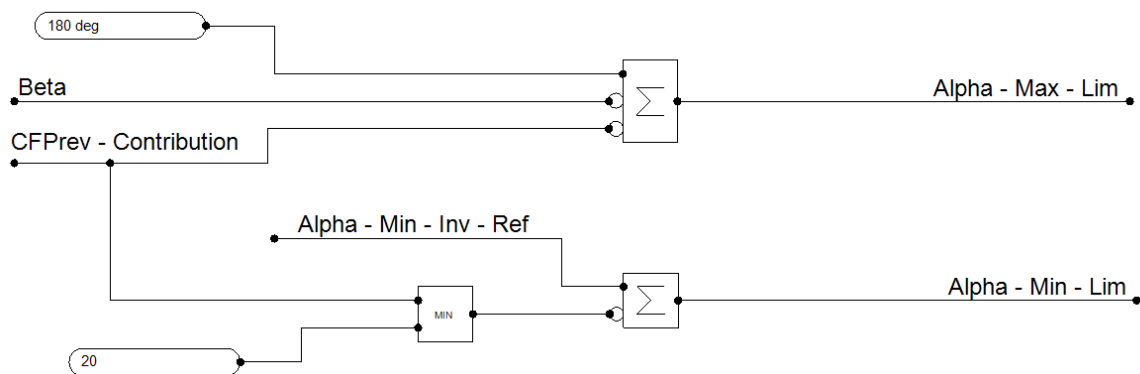


Figure 3.8: Constant beta function

When no output is received from the CFPprev function, the Beta angle is subtracted from 180° to obtain the maximum alpha limit, Alpha - Max - Lim . However, when the CFPprev function is activated, CFPprev-Contribution is then subtracted from 180° to obtain an even lower Alpha - Max - Lim .

The CFPprev-Contribution is also compared to a constant angle, in this case 20° . The minimum value is subtracted from the minimum inverter alpha reference, $\text{Alpha - Min - Inv - Ref}$, to obtain the the minimum alpha limit, Alpha - Min - Lim .

4

Commutation Failure

Commutation failure is an adverse dynamic event that occurs when a converter valve that is supposed to turn off continues to conduct. Hence, the current is not transferred to the next valve in the firing sequence. Its occurrence causes a temporary interruption of transmitted power and stresses the converter equipment [3]. Furthermore, it can result in significant direct current increase and thus lead to additional heating of the converter valves. Consequently, shortening their lifespan [4]. Most commutation failures are caused by voltage disturbances due to AC system faults and they can never be completely avoided [16].

For successful switching of thyristor valves, it's required that the internal stored charges produced during a forward conduction interval must be removed before the valve can establish forward voltage blocking capability [2]. Otherwise, the valve will start to re-conduct even without being fired resulting in an unwanted short-circuit, then a commutation failure may be initiated [4].

When the current in the outgoing valve reaches zero, the valve needs to be deionised. A certain voltage-time area is required for deionisation of the thyristor to remove internal charges built up during conduction. In the unfortunate event that the remaining voltage-time area under the commutation voltage at the end of the overlap is not enough for deionisation, the thyristor will not be able to achieve forward blocking. This remaining voltage-time area after commutation is analogous to the extinction angle, γ .

As mentioned earlier, the commutation process can proceed as long as the commutation voltage is positive. When the converter is operating in rectifier mode, γ is large enough. Therefore, the risk for commutation failures in the rectifier is very low. However, there is a high risk that during inverter operation, the remaining voltage-time area after commutation is too small. Therefore, various disturbances in the connected AC system can greatly affect the normal commutation process resulting into single or multiple commutation failures. Increasing the nominal value of γ during normal inverter operation increases the margin for successful commutation. However, it is desired to keep γ as low as possible to minimise valve losses and costs [9].

Moreover, maintaining a large voltage-time area can be challenging since it means

4. Commutation Failure

a lower voltage output coupled with a higher current. This condition results into increased converter reactive power consumption. The desire to strike a balance between keeping an adequate voltage-time area and the reactive power consumption imposes considerable constraints on the control system [17].

Consider a commutation of current from valve 1 to 3 in figure 2.2. Assuming that after the firing of valve 3 a disturbance occurs in the system which reduces the remaining voltage-time area for valve 1 so that no forward blocking capability is achieved for valve 1. This disturbance affects the normal commutation process and as a result the current through valve 1 increases as the current in valve 3 decreases to zero again; this is commutation failure. The next scheduled commutation is from valve 2 to 4. When valve 4 is fired, a point is reached where valves 1 and 4 are conducting simultaneously and the converter bridge is short circuited on the DC side. The occurrence of a commutation failure leads to a zero voltage across the faulty bridge. Consequently no active power can be transmitted by the converter bridge.

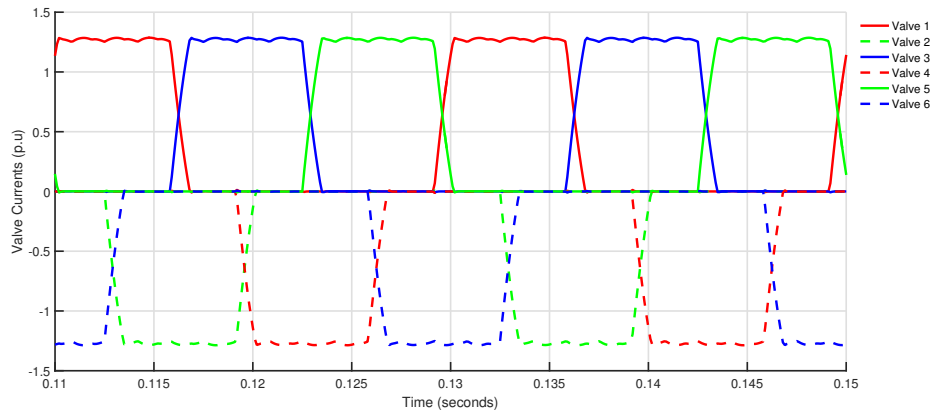


Figure 4.1: Valve currents during successful commutation

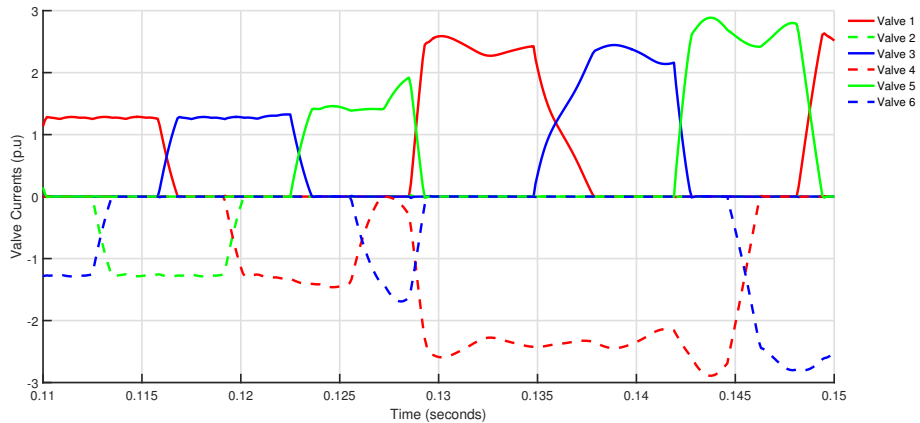


Figure 4.2: Valve currents during a failed commutation

4.1 Causes of Commutation Failure

Commutation failures in HVDC systems mainly occur as a consequence of voltage dips due to AC system faults or switching actions close to the inverter station. Since the AC voltage dips result in both voltage magnitude reduction and phase-angle shift, they may affect the commutation process leading to commutation failures [14].

Basically the occurrence of three events before or during the commutation process could culminate into commutation failures. These events are:

- A decrease in the commutating voltage.
- An sudden increase in the direct current.
- A hardware malfunctioning in the firing control.

Disturbances in the commutating voltage is the most common of all three events, it is attributable to symmetrical and unsymmetrical faults in the connected AC systems and can never be completely avoided [9]. During normal inverter operation, the nominal firing or delay angle is carefully chosen such that a sufficient extinction angle is obtained to avoid commutation failures. However, when there is a sudden change in the system conditions before or during the commutation process, the remaining voltage-time area maybe insufficient for successful commutation.

The symmetrical three phase faults result in a balanced reduction of all phase voltage magnitudes. It however, does not distort the phase angles. The occurrence of these faults leads to a reduction in the AC system voltage as well as a temporary increase of direct current at the inverter station.

Furthermore, unsymmetrical faults which are the most common occurring faults in power systems result in distortions of the resulting commutating voltage. These faults lead to phase angle shifts in addition to a reduction of the commutating voltage magnitude. Moreover, the voltage shape of the commutating voltage is distorted and usually results into a non-sinusoidal commutating voltage. The disturbances in the commutating voltage can also be introduced due to switching operations such as transformer energising in, or close to the inverter station [9].

The second event whose occurrence could lead to commutation failure is a sudden increase in the inverter station direct current. This event is usually due to system faults, but could also be caused by very rapid control system action [9]. An increase in the direct current will increase the time needed for commutating the current. Assuming the firing angle remains unchanged, the extinction angle decreases in accordance with (2.1). In order to guarantee that the remaining voltage-time area is sufficient for successful commutation, the firing angle is adjusted to the new direct current level.

Finally, an internal malfunction of the converter firing control system or an action of the protection function could lead to commutation failure. Failure of the CFC would mean no firing pulse for the next valve in the firing sequence resulting into commutation failure.

4.2 Mitigation of Commutation Failure

Commutation failure occurs if the remaining voltage-time area after a firing is insufficient. Some of the common ways of decreasing the risk of commutation failure are described below.

Operation with a large commutation margin, γ , such that disturbances do not result into commutation failures. In order to decrease the risk of commutation failures, the steady state commutation margin is increased. The larger this margin, the more severe the disturbances can be without commutation failures. However, operation with a higher commutation margin gives a higher cost of equipment and higher losses [9].

Furthermore, commutation failure can be avoided by temporarily increasing the commutation margin just before a planned switching action. This will mitigate against commutation failures associated with scheduled switching. After the scheduled switching, the commutation margin is restored to its steady state value.

Measures such as installation of DC reactors with large inductance can be taken to decrease the rate of change in direct current during the disturbances and/or system faults. The large inductance ensures that the sudden increase of the current due to faults occurs at a relatively slow rate allowing for the commutation process to be completed successfully. If the current increase is ordered by the control system, commutation failures can be avoided by appropriately adjusting the control response.

Commutation failures resulting due to internal failure or malfunction of the HVDC control system, can be avoided by designing high reliability control systems and providing backup systems [9]. Usually a combination of the above measures is employed to reduce the risk of commutation failures in HVDC systems.

4.3 Recovery from Commutation Failure

As stated earlier, an AC system fault on the inverter AC network may result into undesired voltage drops as well as phase shifts. The magnitude of the voltage drop largely depends on the proximity of the fault to the inverter bus. The nearer the fault is to the inverter bus, the larger the voltage drop [8]. The start of failed commutation depends on the phase shift and voltage drop magnitude.

Any single phase to ground fault that causes the inverter AC voltage to drop to approximately 80% or below of its pre-fault value will most likely lead to the start of failed commutation. However, if the fault does not result into a voltage drop of below 90% in any of the phases then there is a chance that no commutation failure will occur [9]. The likelihood of commutation failure for comparable balanced three phase faults is less. This is attributable to the absence of commutating voltage phase shifts.

Modern HVDC systems through their control systems have the ability to successfully recover after the first few failed commutations. Having recovered, they are capable of providing reduced power injection at the low AC voltages before the fault is cleared [9]. As the systems attempt to recover prior to fault clearing, the direct current and DC voltage may have oscillations due to the unbalanced AC voltages.

Furthermore, when the AC fault is very close to the inverter bus such that the voltage drops to near zero, then the chances of recover prior to fault clearing are greatly reduced. In this case, no power injection is possible unless the fault is cleared. The HVDC control and protection schemes influence the system's recovery capabilities.

In some HVDC systems, the AC voltage level is monitored and the valve firing signals blocked when the voltage drops below a certain level. The valve firing signals are only unblocked when the voltage recovers and returns to a desired level. Some other systems do not utilise the blocking of the valve firing signals, instead they employ a mechanism to reduce power injection at reduced voltage levels [9].

The Voltage Dependent Current Limit (VDCL) is one such mechanism. This function may be triggered during repeated commutation failures to safeguard the converter valves and improve the HVDC system's performance during recovery after failed commutation [6].

5

Commutation Failure Detection and Prevention

The methodology adopted and the simulations performed for the thesis project are described in this chapter. Firstly, a base simulation model of an HVDC system was modified to suit the objectives of the thesis project. The functionality of the modified model was checked and all issues discovered resolved.

The thesis project was then subdivided into the following key tasks;

- Analysis of the existing commutation failure prevention (CFPrev) function with special emphasis on the triggering and the operation of the function.
- Execution of a dynamic performance study to determine which of system disturbances and/or faults return poor results with the existing CFPrev function.
- Development and implementation of an improved CFPrev function based on area contribution instead of angle contribution.
- Execution of a similar dynamic performance study to check for any improvements or deterioration in the CFPrev performance.
- Testing of the proposed CFPrev function for different AC network Short Circuit Ratios (SCR).
- Optimisation of the proposed CFPrev function.

All the above tasks were performed so as to facilitate the successful completion of the thesis project.

5.1 Simulation Model

A bipolar HVDC configuration PSCAD model shown in Fig. 5.1 was used for this thesis. The simulation model consists of two converter stations with each converter station is composed of two poles. One station was operated in rectifier mode while the other station was operated in inverter mode. Each pole was made up of two series connected six pulse bridges, forming a twelve pulse converter bridge.

AC filters, smoothing reactors and shunt capacitors are connected to each pole, and the filters were tuned to suppress the AC harmonics. The two converter stations are connected to each other through an overhead DC transmission line with a DC resistance of $0.05\Omega/\text{Km}$. Each converter station was connected to a different AC network. The AC networks were modeled in PSCAD using three phase voltage sources behind an impedance.

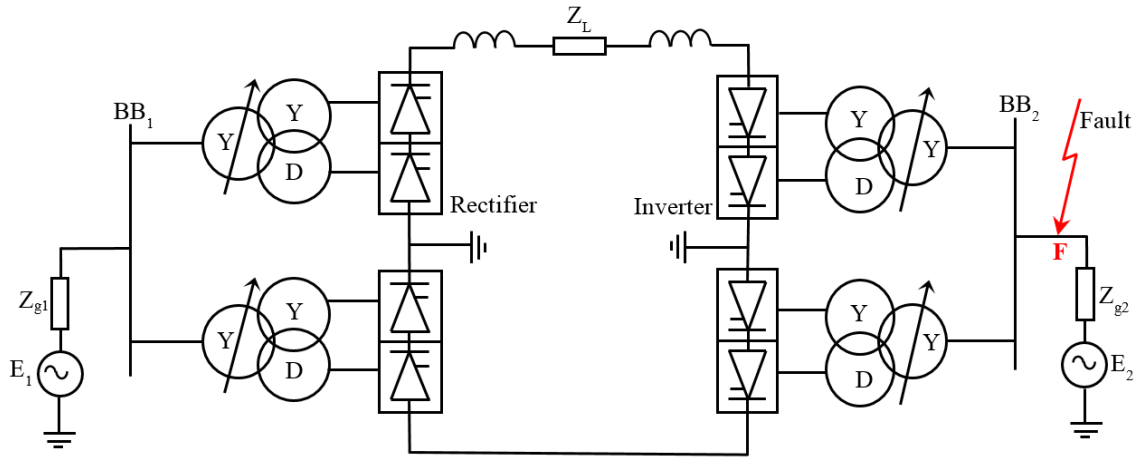


Figure 5.1: The simulation model setup

As is shown in Fig. 5.1, the rectifier AC network was modeled by a voltage source, E_1 behind an impedance Z_{g1} while the inverter AC network was modeled by a Voltage source, E_2 behind an impedance Z_{g2} . BB_1 and BB_2 represent the rectifier and inverter AC bus-bars respectively.

The simulation model parameter settings for both rectifier and inverter stations are given in Table. 5.1.

Table 5.1: Simulation model parameter settings.

Parameter [Unit]	Rectifier	Inverter
AC system frequency [Hz]	50	50
AC system Voltage [p.u.]	1.06	1.03
Rated power [p.u.]	1	1
Rated current [p.u.]	1	1
Nominal firing angle [deg]	15	-
Minimum firing angle [deg]	5	110
Nominal extinction angle [deg]	-	17
Minimum valve extinction time [μs]	445	445
Nominal reactive DC voltage drop [p.u.]	0.07	0.07
Nominal resistive DC voltage drop [p.u.]	0.00209	0.00209

5.1.1 AC Network Model

In order to investigate the influence of the AC network short circuit capacity on the operation of the CFP_{prev} function, four AC networks of different short circuit ratios were studied. The AC network short circuit capacities were varied by changing the AC grid impedance. SCR can be calculated as,

$$SCR = \frac{S_{cp}}{P_n} \quad (5.1)$$

, where S_{cp} is network short circuit power and P_n is the nominal power of the converter station. The AC networks were modeled with SCR of 3, 4, 5 and 7. For this thesis project, networks with SCRs between 5 and 7 were considered as a strong network while the network with the SCR of 3 was treated as a weak network. The impedance settings for the SCRs studied are shown in Table. 5.2.

Table 5.2: Impedance values for different SCRs.

SCR	Z_{g1} [p.u.]	Z_{g2} [p.u.]	Impedance angle [deg]
3	0.00033	0.00033	83.15
5	0.00020	0.00020	83.15
7	0.00014	0.00014	83.15
10	0.00010	0.00010	83.15

5.1.2 AC system disturbances

Since majority of commutation failures occur as a result of voltage dips caused by AC faults, different AC system faults were initiated. This was done to study the failed commutations that could occur as well as to investigate the performance of the existing and proposed CFP_{Prev} functions. Moreover, it provided the basis for comparing the two functions.

Single phase to ground faults (the most commonly occurring AC faults) and three phase to ground faults (the most severe AC faults) were applied on the inverter AC network at point F in Fig. 5.1. Prior to fault initiation, a steady state operating point was determined and the pre-fault AC voltage noted. The faults were applied for a duration of 100ms. The fault impedance was tuned such that a desired remaining AC voltage during the application of the fault is achieved. The remaining voltage was defined as a percentage of the pre-fault voltage. Faults with remaining voltage ranging from 92% to 80% (the faults resulted in a 8% to 20% reduction in the pre-fault voltage) were applied.

5.2 Existing CFP_{Prev} Function

The existing commutation failure prevention (CFP_{Prev}) function consists of two different parts: The predictor that acts when the risk of commutation failure is increased and the detector that acts when a commutation failure has already occurred with the objective of preventing further commutation failures.

With the detection of AC faults and/or commutation failure, the existing CFP_{Prev} function outputs an angle contribution. This angle contribution is then used to increase the $A_{min-ref-final}$ (see Fig. 3.7) and results in an earlier firing, preventing a commutation failure from occurring or further commutation failures if one has already occurred. The angle contribution is also sent to Constant Beta function to cause a reduction in the maximum and minimum alpha limitations (see Fig. 3.8).

Commutation Failure Prediction (CFP_{Pred})

In order to prevent commutation failures due to AC faults as well as other system disturbances that result into reduced AC voltages, this function is used. The function comprises of two parallel parts namely zero sequence detection and alpha-beta detection.

The first part is based on zero-sequence detection to identify the occurrence of asymmetrical (unbalanced) faults whereas the second part is based on α/β transformation of the AC voltages with the aim of detecting the occurrence of symmetrical (balanced) faults.

The detection principles are based on the fact that for asymmetrical faults, the sum of the three AC voltages will differ from zero whereas for symmetrical faults, the output vector from the abc to $\alpha\beta$ transformation will be smaller in magnitude compared to the output vector during normal operation conditions. The block diagram in Fig. 5.2. shows the CFPred function design.

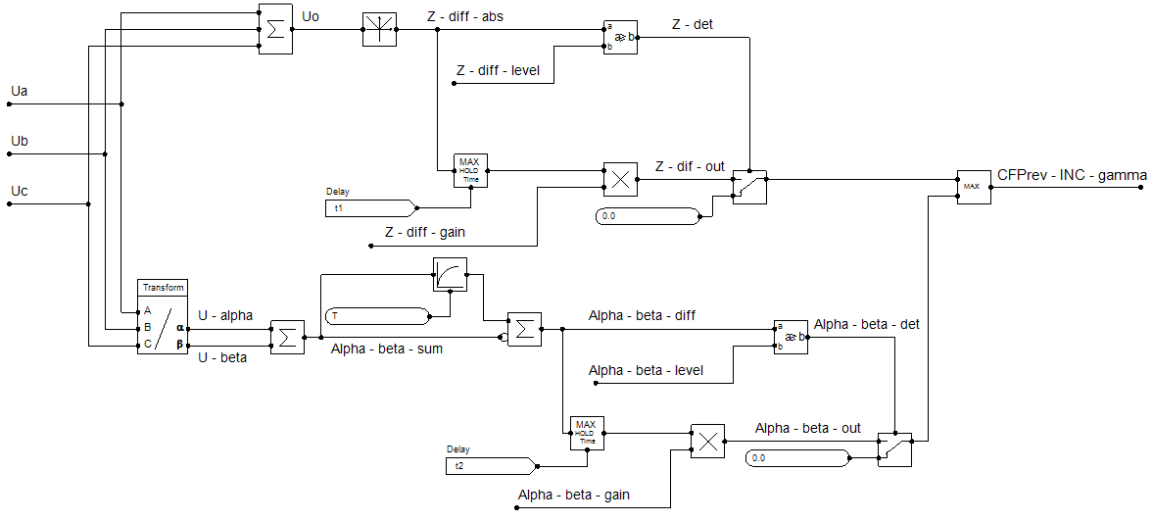


Figure 5.2: Commutation failure prediction function (CFPred)

U_o is obtained simply by summing up the three phase instantaneous voltages as in (5.2).

$$U_o = U_a + U_b + U_c \quad (5.2)$$

The absolute value of U_o , $Z - diff - abs$ is obtained and sent to the max-hold block. The max-hold function is used to convert the sinusoidal wave shape into a DC quantity. The max-hold block is designed such that it stores the maximum value it detects and keeps it for a certain time, if no larger value is detected. The delay time is determined by the value of t_1 . The output from the max-hold block is then multiplied by the $Z - diff - gain$ to obtain $Z - diff - out$.

If absolute value of U_o is greater than a predefined level ($Z - diff - level$), the signal $Z - det$ is activated. This signal turns on the switch consequently transmitting $Z - diff - out$ to the max block. In the event that no contribution is received at the max block from the $\alpha\beta$ part, $Z - diff - out$ then represents the angle contribution that will be subtracted from the final firing angle to prevent commutation failure.

The second part of CFPred is based on abc to $\alpha\beta$ transformation to detect symmetrical and three phase faults. The transformation from abc to $\alpha\beta$ enables the use of one rotating vector to represent the three phase instantaneous voltages. The use of one rotating vector simplifies the analysis of the AC voltages since one degree of

freedom is eliminated [2]. Moreover, the transformation makes it straightforward to identify transients and other AC system disturbances. The expressions of U_α (U-alpha) and U_β (U-beta) used in CFPred function are given by (5.3) and (5.4) respectively.

$$U_\alpha = \frac{2}{3}U_a - \frac{1}{3}(U_b + U_c) \quad (5.3)$$

$$U_\beta = \frac{\sqrt{3}}{3}(U_b - U_c) \quad (5.4)$$

U_α and U_β correspond to the projection of the vector $U_{\alpha\beta}$ on the $\alpha\beta$ plane. The transformation of symmetrical three phase quantities gives a rotating vector in the $\alpha\beta$ plane. The quantity *alpha-beta-sum* in Fig. 5.2. is calculated by (5.5), which equals the magnitude of the rotating vector.

$$|U_{\alpha\beta}| = \sqrt{U_\alpha^2 + U_\beta^2} \quad (5.5)$$

Alpha-beta-sum will give a DC value when the three phases of the AC inverter bus voltage are symmetrical [2]. The *alpha-beta-sum* is subtracted from a filtered *alpha-beta-sum* to give the *alpha-beta-diff* value. The filtered value acts as the pre-fault voltage and the filter time constant is determined by the time setting T .

The *alpha-beta-diff* value in Fig. 5.2 then forms an input to the max-hold function. The max-hold function is used on the *alpha-beta-diff* although this is assumed to be a DC value during a balanced three phase fault. This is so because the *alpha-beta-diff* has transient oscillations immediately after fault initiation. Furthermore, during an unbalanced fault, *alpha-beta-diff* is an oscillating value due to the presence of a negative sequence component. Therefore, the max-hold is necessary in order to transform it into a DC quantity. The output from the max-hold block is multiplied by the *alpha-beta-gain* to give *alpha-beta-out*.

During normal operation, the *alpha-beta-diff* value is approximately zero. However, when a disturbance occurs in the AC system, it will be non-zero. The non-zero value indicates that an AC voltage dip has occurred at the inverter bus. The obtained *alpha-beta-diff* value is compared with the pre-determined *alpha-beta-level*. If the *alpha-beta-diff* value is greater than or equal to the *alpha-beta-level*, the signal *alpha-beta-det* is activated and it turns on the switch. With the switch turned on, *alpha-beta-out* is then sent to the max block. In the event that there is no contribution from the zero sequence part, *alpha-beta-out* represents the angle contribution that will be subtracted from the final firing angle to prevent commutation failure.

Despite the fact that the two parts of CFPred detect different fault conditions, both could be activated at the same time. When this happens, the max block compares the *Z-diff-out* and *alpha-beta-out* values. It then outputs *CFPrev-INC-gamma*, the larger of the two values which then gives the final output of the entire control function. The *CFPrev-INC-gamma* value will be subtracted from the final inverter firing angle. This results in advancing the firing instant and leaving a margin sufficient enough for successful commutation.

Commutation failure Detection (CFDET)

The commutation failure detection acts when the predictor has failed to prevent a commutation failure. A commutation failure is detected by comparing the DC with the AC current on the valve side of the transformer. If a commutation failure occurs, the current on the DC side will increase and the current on the AC side will decrease. This function is set up and designed basing on a six-pulse bridge as shown in Fig. 5.3.

The valve currents flowing through the six-pulse bridge connected to the wye winding of the converter transformer are monitored and compared. The valve currents flowing through the six-pulse bridge connected to the delta winding of the converter transformer are also monitored and compared. $Max - IVY$ in Fig. 5.3 is the maximum valve current obtained from the wye group while $Max - IVD$ is the maximum valve current from the delta group.

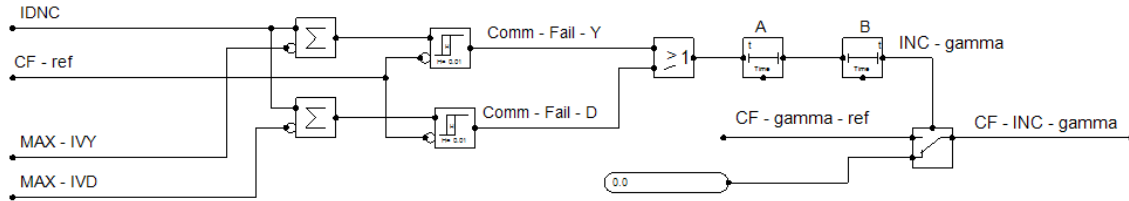


Figure 5.3: Commutation failure detection function

$Max - IVY$ and $max - IVD$ are subtracted from the nominal direct current, $IDNC$ to give current errors. The current errors are then compared with $CF-ref$, a predefined error level, in a hysteresis block. If the conditions in the upper hysteresis block (see Fig. 5.3) are satisfied, a $comm - fail - Y$ signal is outputted signifying a commutation failure in the wye group. If the conditions in the lower hysteresis block (see Fig. 5.3) are satisfied, a $comm - fail - D$ signal is outputted signifying a commutation failure in the delta group.

Since only one of $comm - fail - Y$ or $comm - fail - D$ is required to indicate commutation failure, the two signals are sent through to an OR block. The output from the OR block is sent to a delay on block, A . In this block the output remains low for a given time after the input has gone high. The output from the delay on block is sent to a delay off block, B . In this block the output remains high for a given time after the input has gone low. When the output from the delay off block, $INC - gamma$, is high, the switch in Fig. 5.3 is turned on and the value $CF - gamma - ref$ is transmitted as the output ($CF - INC - gamma$) of the commutation failure detection function.

When a commutation failure is detected in one bridge, $CF - INC - gamma$ (a contribution from CFDet) is added to the extinction angle before the next firing to prevent any commutation failures in the next bridge.

The outputs from the commutation failure prediction and detection functions are combined to give the final output from the commutation failure prevention function. Fig. 5.4 shows combination of the two values. When the prediction function (CFPred) is activated, the value $CFPrev - INC - gamma$ is non-zero conversely when the detection function (CFDet) is activated, the value $CF - INC - gamma$ is also non-zero.

$CFPrev - INC - gamma$ together with $CF - INC - gamma$ are angular values in radians and form the inputs to the max block where they are compared and the larger of the two forms the output of the block.

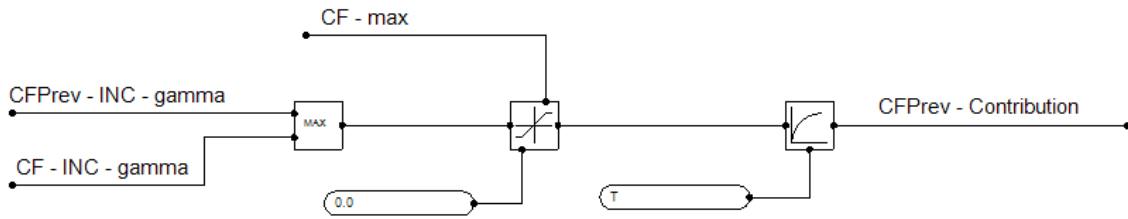


Figure 5.4: Commutation failure prevention function

The output from the max block is kept within zero and $CF - max$, these limits are necessary to maintain the stability of the CFPred function. Without the limits, the activation and operation of the commutation failure prevention function could lead to further commutation failures instead of preventing them. The output from the limit block is passed through a filter to obtain the final output, $CFPrev - contribution$, from the commutation failure prevention function.

$CFPrev - contribution$ then forms an input to both the Constant Beta and Area Minimum control blocks. In the Constant Beta control block it is used to lower the maximum firing angle limit to allow for earlier firing of the converter valves. While in the Area Minimum block it is used increase the minimum voltage-time area, below which emergency firing would normally be activated.

5.3 Proposed CFPprev function

The idea was to design and implement a CFPprev function based a voltage-time area contribution instead of an angular contribution as is the case with the existing function. Fig. 5.5 shows the proposed changes to the existing CFPprev function to facilitate the design of an area contribution based function.

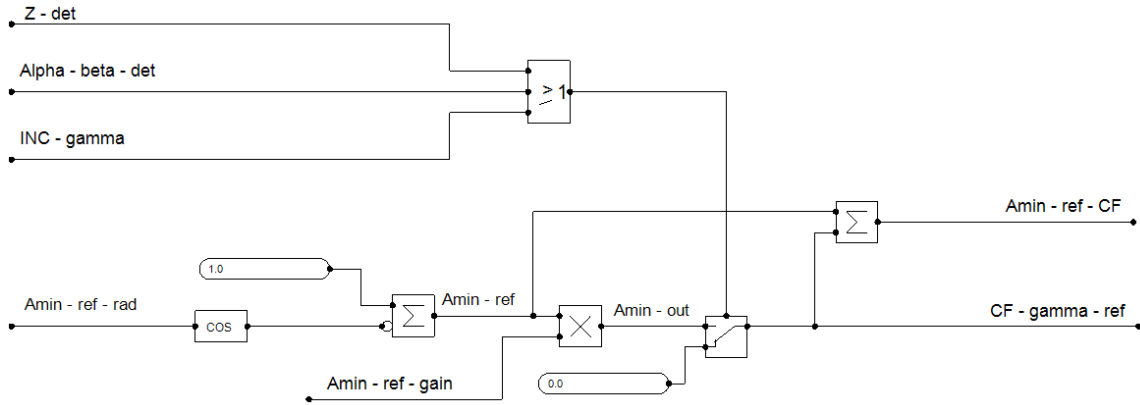


Figure 5.5: Proposed changes to the CFPprev function

No changes were made to the existing prediction and detection functions. The angular value $Amin - ref - rad$, which is the minimum value the extinction angle is allowed to reach before emergency firing is activated, is converted into an area value $Amin - ref$. This area is then multiplied by a variable gain, $Amin - ref - gain$, to give $Amin - out$.

The signals $Z - det$ and $alpha - beta - det$ (see Fig. 5.2) from the prediction function as well as the signal $INC - gamma$ (see Fig. 5.3) from the detection function are used to activate the switch. Once the switch is activated, $Amin - out$ is transmitted through to give the value $CF - gamma - ref$, which is used in the CFDet function. $Amin - out$ is also added to the $Amin - ref$ to give the $Amin - ref - CF$.

$Amin - ref - CF$ then forms the input to the area-min control block where it's used to increase the minimum voltage-time area, below which emergency firing would normally be activated. $CF - gamma - ref$ is transmitted through a filter and limit block before it's sent to the Constant Beta control block.

The optimisation of the proposed CFPprev function is done by studying the performance of the function when the HVDC system is subjected to different fault conditions. This was done while varying the fault initiation time, fault duration and the inverter AC network short circuit ratio. For all cases, the value of the $Amin - ref - gain$ required to prevent the occurrence of a commutation failure or further commutation failures was noted.

6

Results and Discussions

This chapter contains results from the simulations performed using the PSCAD simulation model described in section 5.1.

Firstly, the simulation model of the HVDC system was given controls containing the existing CFPrev function. The AC network parameters were tuned to give the desired network SCR. For a given simulation case, the same SCR was used for both the rectifier and inverter AC networks.

Next, the steady state operation point of the system was established and a snapshot taken and saved. This snapshot was taken after 10s (simulation time within PSCAD). A series of single phase to ground faults and three phase to ground faults were then applied to the inverter AC system. The faults resulted in a 8% to 20% reduction in the pre-fault voltage.

During the fault simulation the start-up method within PSCAD was set to start from the earlier obtained steady state snapshot. Generally, the faults were initiated after 100ms unless stated otherwise.

Secondly, the simulation model was given controls containing the proposed CFPrev function. All the other control parameters were kept constant. The procedure described in the above paragraphs was then repeated. During the simulations the parameter, Amin-ref-gain (see Fig. 5.5), was varied to check the performance of the proposed CFPrev function.

In sections 6.1 and 6.2, the value of Amin-ref-gain (see Fig. 5.5) for the proposed CFPrev function was kept constant at 0.8 for all simulated fault cases. This was done to ensure that the conditions remained the same to provide an equal basis for comparison of the results.

Table. 6.1. contains the description of the variables presented in the results.

Table 6.1: Variables presented in the results

Variable [Unit]	Description
UAC_S1_1 [p.u.]	Phase 1 rectifier network AC voltage
UAC_S1_2 [p.u.]	Phase 2 rectifier network AC voltage
UAC_S1_3 [p.u.]	Phase 3 rectifier network AC voltage
UAC_S2_1 [p.u.]	Phase 1 inverter network AC voltage
UAC_S2_2 [p.u.]	Phase 2 inverter network AC voltage
UAC_S2_3 [p.u.]	Phase 3 inverter network AC voltage
Id_S1 [p.u.]	Rectifier direct current
Iord_S1 [p.u.]	Rectifier direct current order
Id_S2 [p.u.]	Inverter direct current
Iord_S2 [p.u.]	Inverter direct current order
Ud_S1 [p.u.]	Rectifier DC voltage
Ud_S2 [p.u.]	Inverter DC voltage
Pd_S1 [p.u.]	Rectifier DC power order
Pdc_S1 [p.u.]	Rectifier DC power
Pd_S2 [p.u.]	Inverter DC power order
Pdc_S2 [p.u.]	Inverter DC power
Alpha_Meas_S1 [deg]	Rectifier measured firing angle
Alpha_Ord_S1 [deg]	Rectifier ordered firing angle
Alpha_Meas_S2 [deg]	Inverter measured firing angle
Alpha_Ord_S2 [deg]	Inverter ordered firing angle
Gamma_S2 [deg]	Inverter extinction angle
Overlap_S2 [deg]	Inverter overlap angle
D_Valve_Voltage [p.u.]	Inverter Delta group valve voltage
Y_Valve_Voltage [p.u.]	Inverter Wye group valve voltage
Alpha_Beta_diff [deg]	Value of the inverter AC voltage dip
Z_diff_abs [deg]	Magnitude of the inverter zero sequence voltage
Amin_CFPprev [radians]	Output from the CFPprev function

6.1 AC Faults

The simulation results obtained when single phase to ground and three phase to ground faults were applied are presented in this section. The figures shown fall into three general categories.

6.1.1 Strong Network

The results presented in this section were obtained from simulations where both the rectifier and inverter AC networks were tuned to have SCRs of 5.

6.1.1.1 Single phase to ground faults

A single phase to ground fault with a remaining voltage of about 84% was applied on the inverter side. The obtained results from the rectifier side with the existing CFPREV function are presented in Fig. 6.1. The figure consists of five sub-figures. The first illustrates the three phase AC network voltages in per unit, the second contains the direct current (I_d) and the current order (I_{ord}). The third sub-figure shows the DC voltage (U_d) while the fourth contains the DC power order (P_d) and the measured DC power (P_{dc}). Finally, the fifth sub-figure shows the measured firing angle (α_{Meas}) and the ordered firing angle (α_{Ord}).

The occurrence of this fault leads to the distortion of the AC voltages on the rectifier side which consequently results into the rectifier DC voltage drop. Due to the fault current in the AC network, the direct current, I_d starts to increase.

The rectifier responds to the reduction in the DC voltage by increasing its firing angle. This action is expected since the rectifier is controlling the direct current and it seeks to keep the direct current constant. The increase in the firing angle is seen in Fig. 6.1 where both the (α_{Meas}) and the (α_{Ord}) start to rise.

As the DC voltage continues to drop, it reaches a level at which the VDCOL function discussed in section 3.3.1 is activated. When the VDCOL function is activated, it starts to lower the current order, I_{ord} so as to minimise the DC power transmitted during the fault. The DC voltage reaches the lower setting of the VDCOL, at this point, the function maintains the current order at a constant value. The system then starts to recover, (α_{Meas}) and angle (α_{Ord}) begin to decrease and the DC voltage begins to rise.

Although the fault has not yet been cleared, the system recovery starts. The fault is eventually cleared at 0.2s and the system recovery continues successfully. At about 0.3s, the DC voltage and power are both restored to their pre-fault values. The behaviour of the main circuit parameters in the rectifier station was similar for all

6. Results and Discussions

single phase to ground fault cases investigated.

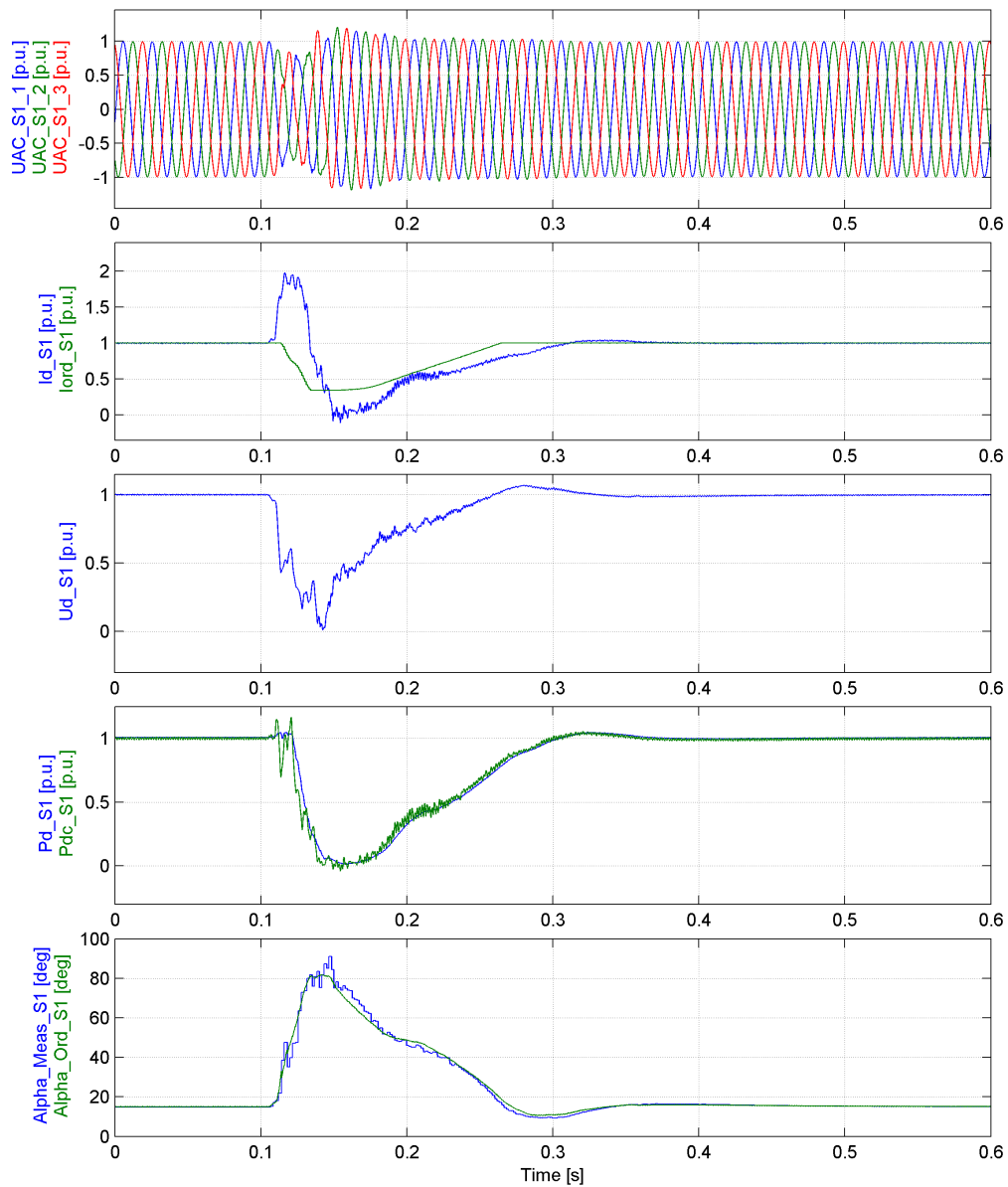


Figure 6.1: Single phase to ground fault with 84% remaining voltage, existing CF-Prev function, Rectifier.

The obtained results from the inverter side with the existing CFPrev are presented in Fig. 6.2. In addition to the five sub-figures described in section 6.1.1.1, the inverter figures have a sixth sub-figure showing the extinction (Gamma) and overlap angles.

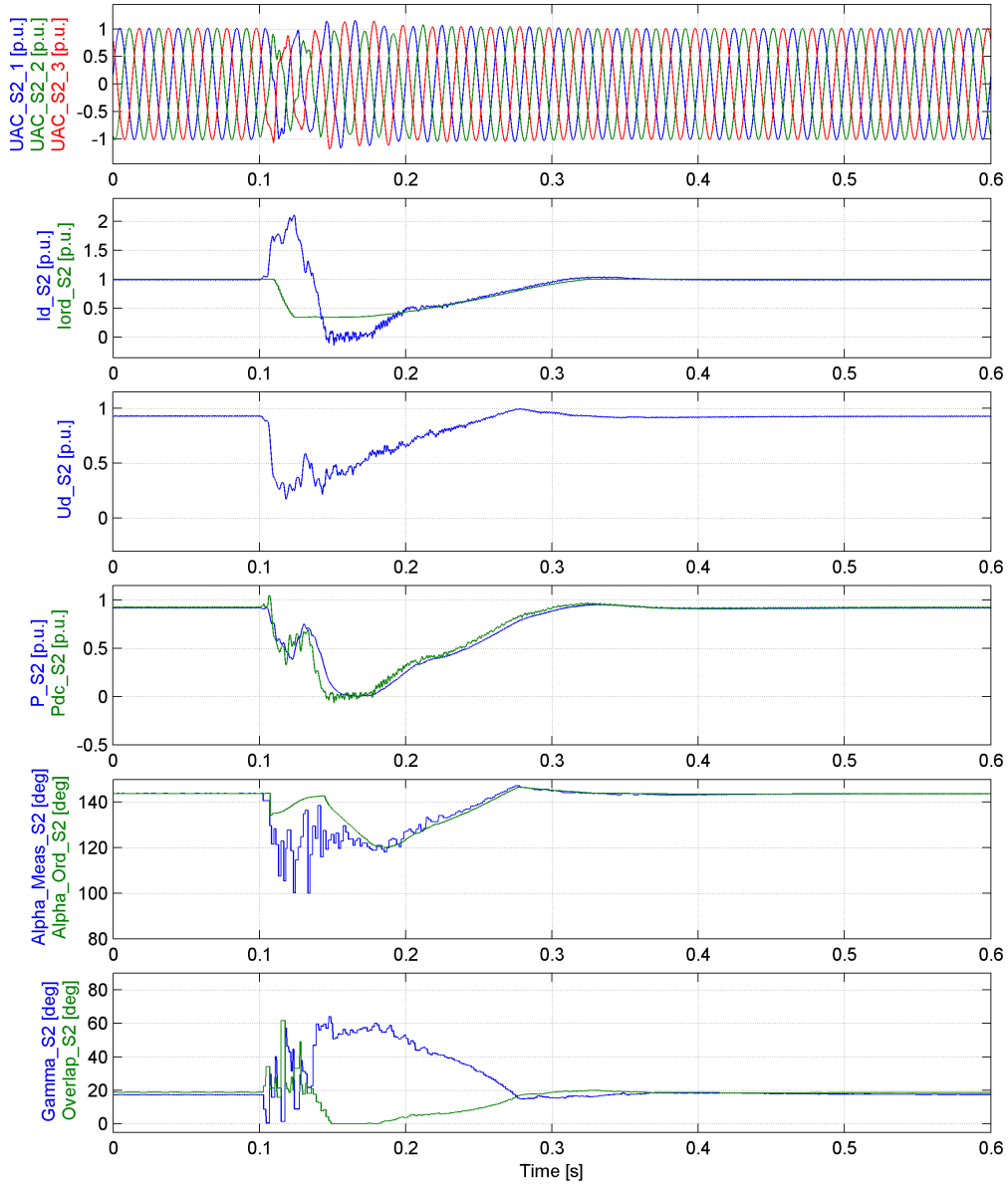


Figure 6.2: Single phase to ground fault with 84% remaining voltage, existing CF-Prev function, Inverter.

The main circuit parameters, the firing, extinction and overlap/commutation angles from the inverter station are presented in Fig. 6.2. When the single phase fault is applied at 0.1s, the AC voltages are distorted in phase and reduced in magnitude. This consequently results into reduced DC voltage. Due to the occurrence of the fault, the alternating current on the inverter side increases hence the inverter direct

current also increases. Since the overlap angle is directly proportional to the direct current, it also starts to increase.

In order to maintain the system DC voltage, the inverter control system responds to the fault by decreasing the extinction angle. This action makes the inverter very susceptible to commutation failures. As the overlap angle increases and the extinction angle decreases, the firing angle also decreases so as to keep the angle balance (see (2.1)). The VDCOL then activates and the recovery is initiated. As the direct current decreases, the overlap angle also decreases.

Fig. 6.3. contains four sub-figures. The first showing the delta group valve voltages (D_valve_voltage) and the wye group (Y_valve_voltage) valve voltages. The second contains the value of the inverter AC voltage dip (Alpha_Beta_Diff) while the third contains the magnitude of the inverter zero sequence voltage (Z_diff_abs). The final sub-figure shows the output from the CFPrev function (Amin_CFPprev)

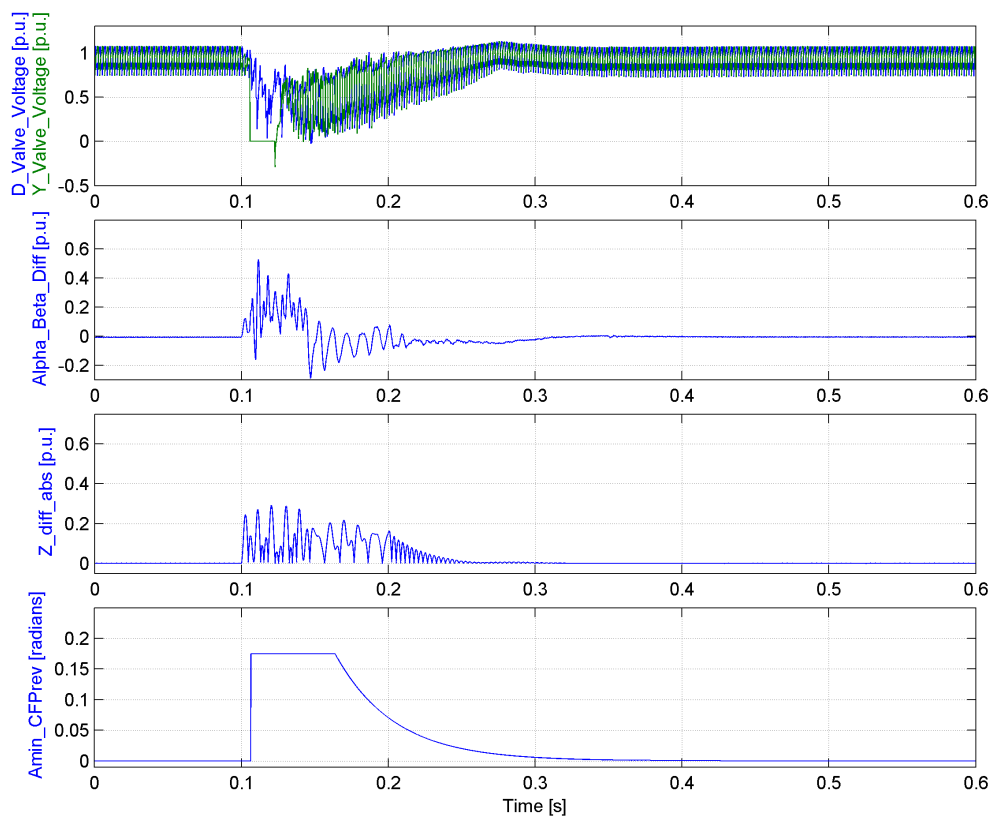


Figure 6.3: Single phase to ground fault with 84% remaining voltage, existing CFPrev function, Inverter.

The delta group and wye group valve voltages as well as the alpha_beta_diff and z_diff, used to detect the occurrence of faults, are shown in Fig. 6.3. Also, shown in this figure is the CFPrev function output. After the fault inception, the wye group valve voltage drops to zero signaling the occurrence of commutation failure

within this valve group. The existing CFPrev function acted however, it was unable to mitigate this particular commutation failure. After a few cycles, the wye group valves were able to re-establish commutation and the system started to recover before the fault was cleared. When the fault was cleared, the system continued to recover and reached steady state at about 320ms.

Proposed CFPrev Function

When a single phase to ground fault with a remaining voltage of approximately 84% was applied, with the proposed CFPrev function in place, no failed commutations occurred. The AC voltages in Fig. 6.4 show a slight drop in magnitude but no phase distortion. The direct current experiences a small increase for about 50ms and returns to approximately its pre-fault value. The DC voltages drops slightly and is oscillatory in nature throughout the fault duration. This is attributable to the resonance developed in the system as a consequence of the single phase to ground fault.

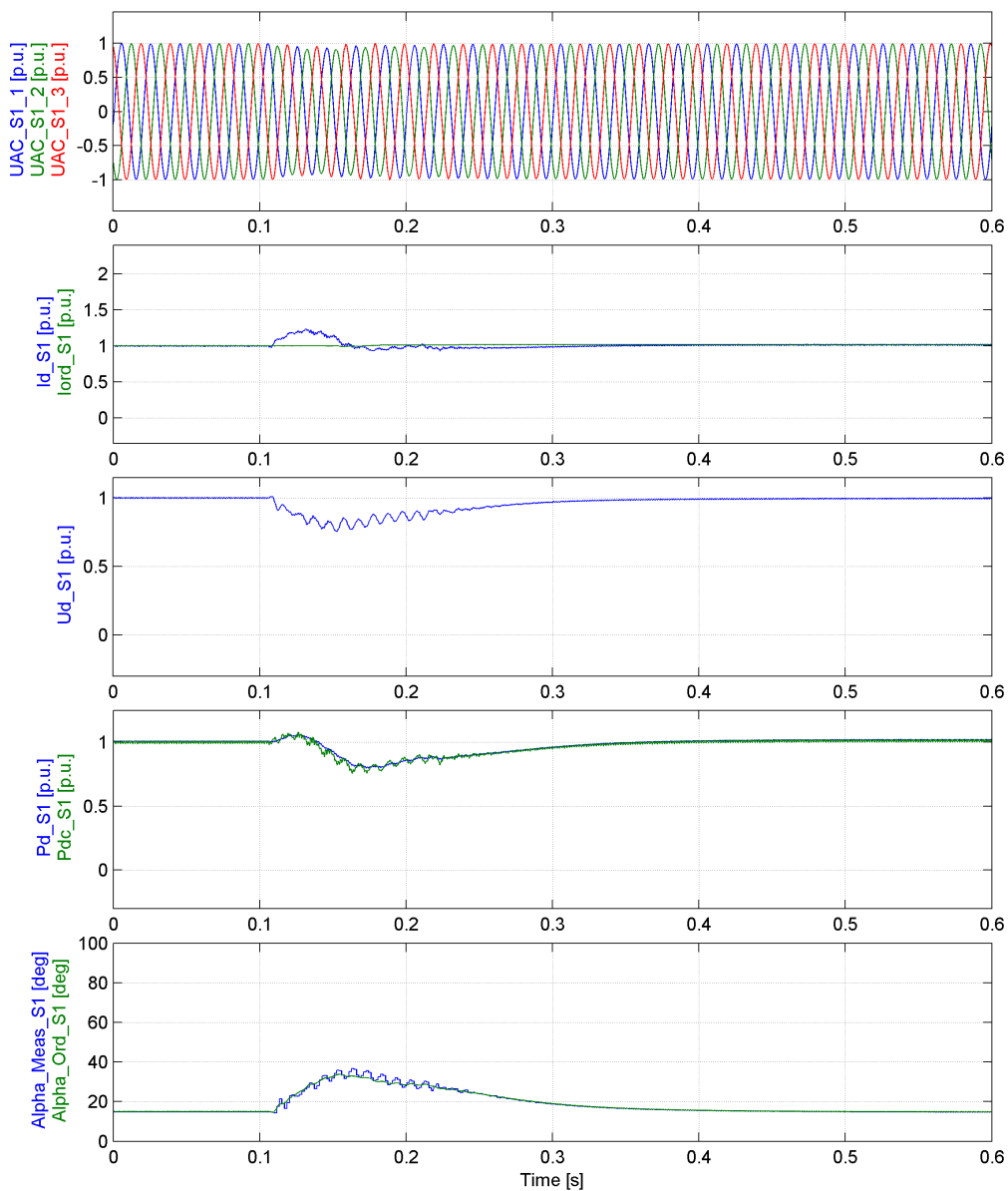


Figure 6.4: Single phase to ground fault with 84% remaining voltage, proposed CFPrev function, Rectifier.

The DC power largely follows a similar trend as the DC voltage while the firing angle increases such that the rectifier is able to maintain a constant current order. It should be noted that the VDCOL function is not activated for this case because the DC voltage does not drop below the set level.

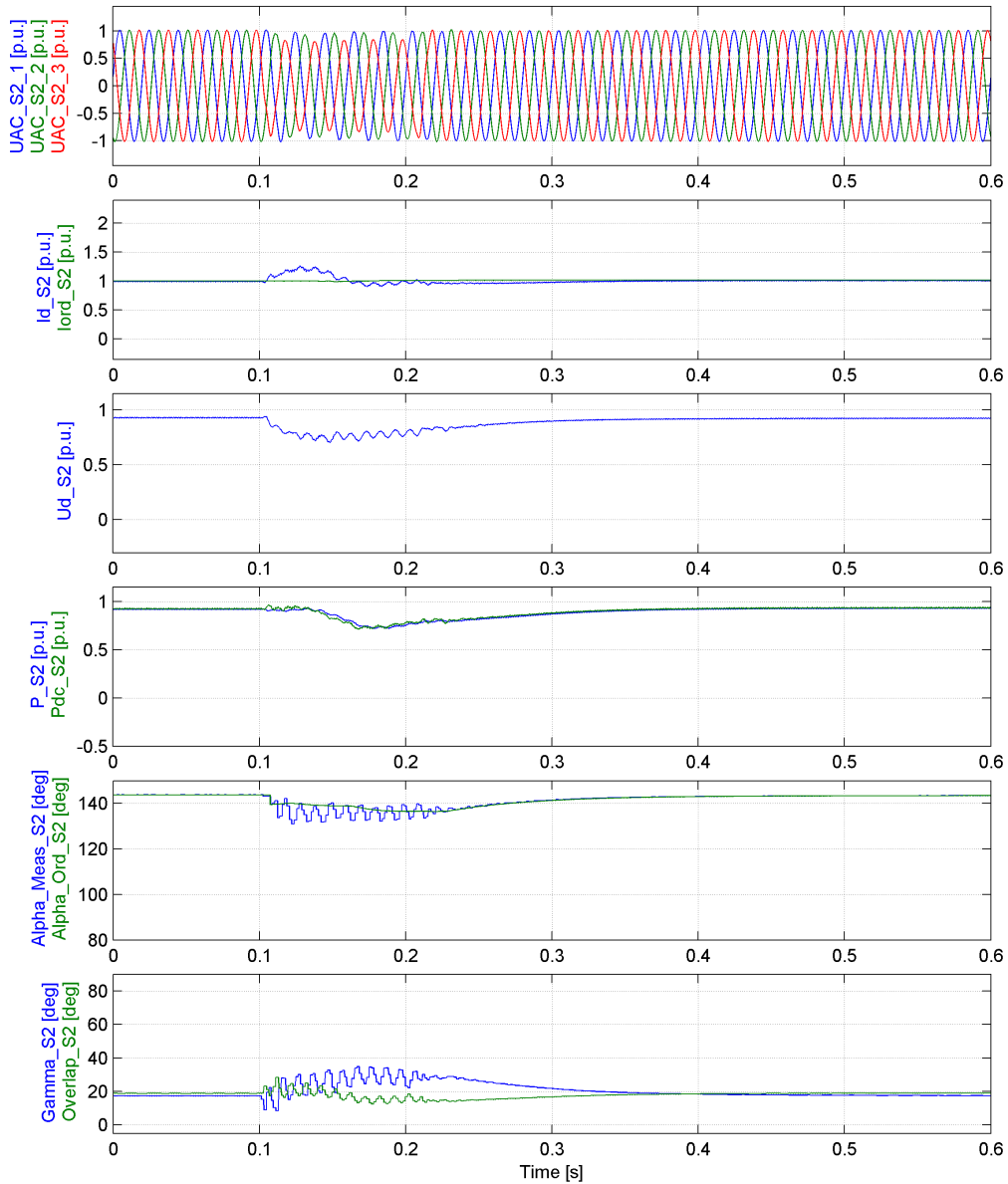


Figure 6.5: Single phase to ground fault with 84% remaining voltage, proposed CFPrev function, Inverter.

The AC voltage, direct current, DC voltage and DC power shown in Fig. 6.5 on the inverter side behave in a similar way as those on the rectifier side shown in Fig. 6.4. The inverter responds to the decrease in voltage by lowering the firing angle so as to raise the extinction angle.

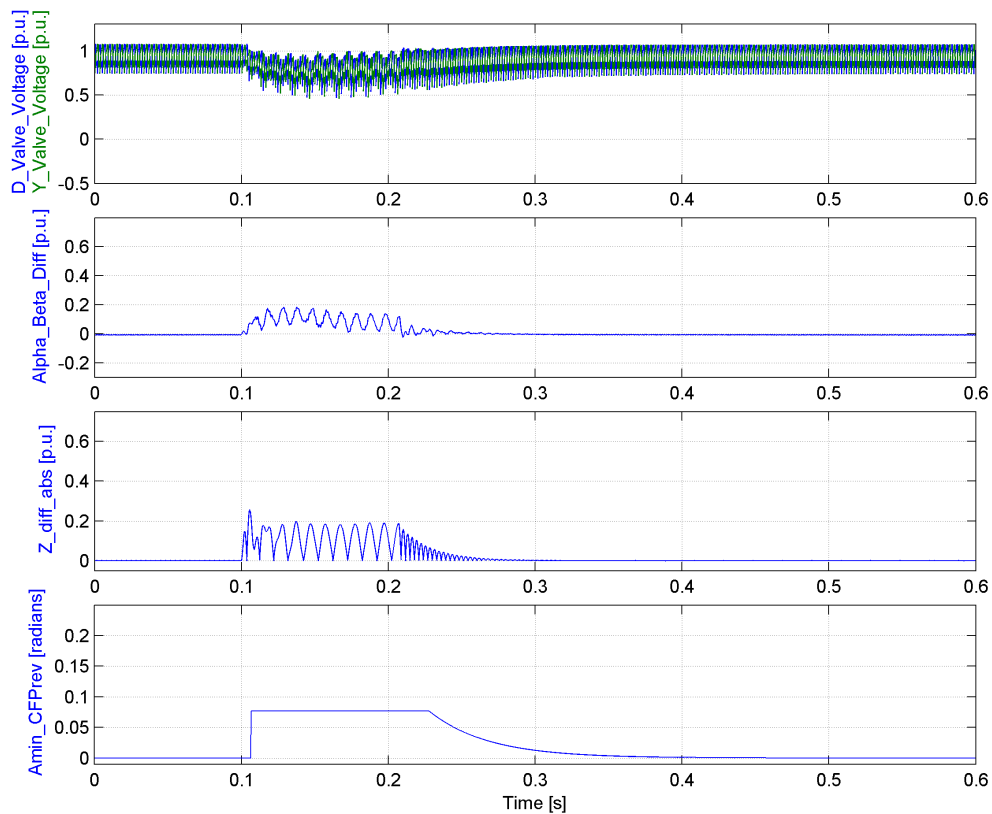


Figure 6.6: Single phase to ground fault with 84% remaining voltage, proposed CFPprev function, Inverter.

In Fig. 6.6, it's clear that the proposed CFPprev acted and was able to mitigate the commutation failure that occurred while the existing CFPprev was utilised. The absence of failed commutation is confirmed since no valve group voltage drops to zero after fault inception. In Fig. 6.3, it can be seen that CFPprev is active for less than 100ms while in Fig. 6.6, CFPprev is active for approximately 150ms. The proposed CFPprev was able to prevent failed commutation due to its longer active time. The fault was cleared after 200ms and the system returned to steady state at about 300ms.

6.1.1.2 Three phase to ground faults

Existing CFPprev Function

When a three phase to ground fault with a remaining voltage of about 85% was applied to the inverter AC network, commutation failure was observed. In this case, the fault was initiated at 102ms and applied for 100ms.

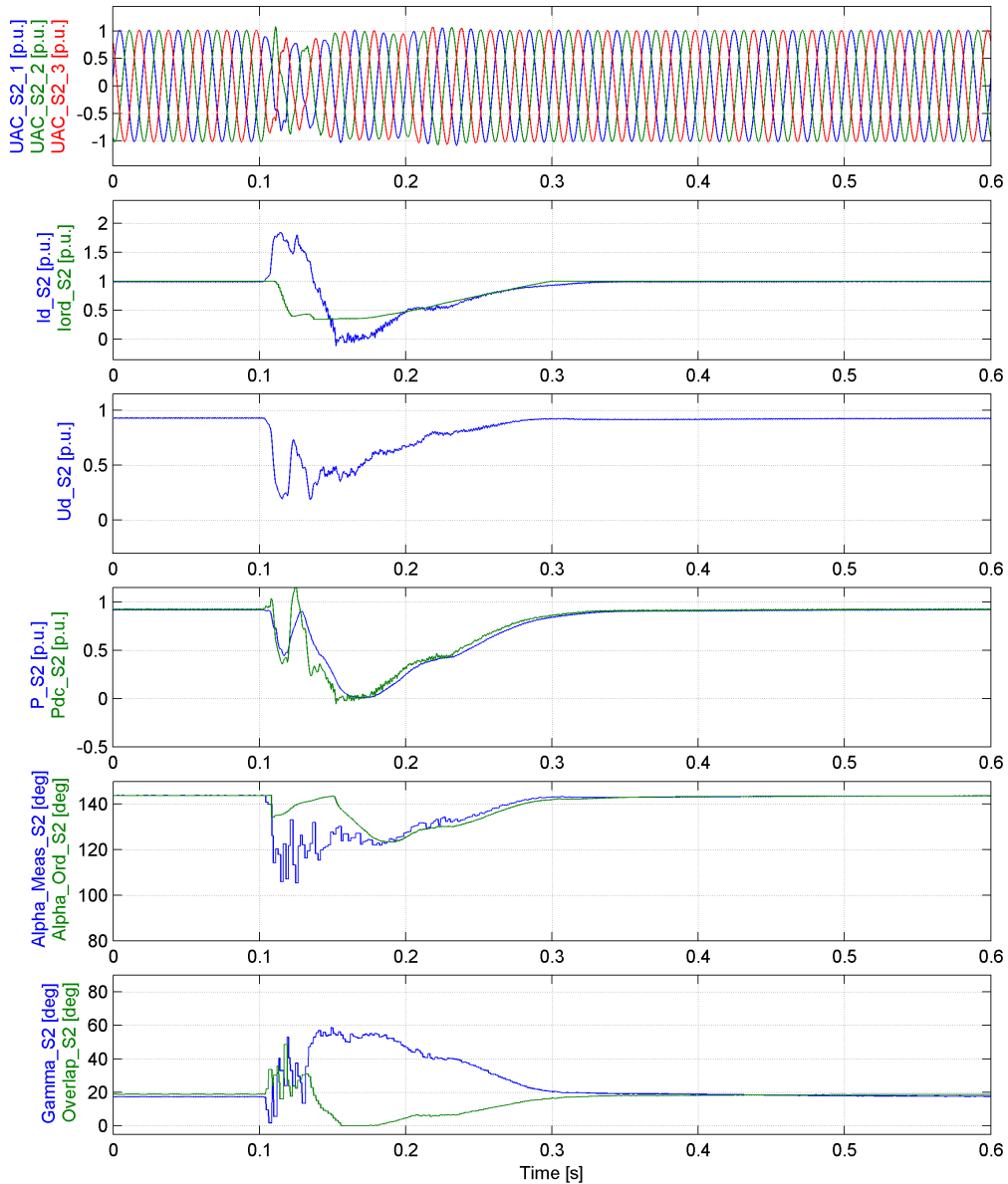


Figure 6.7: Three phase to ground fault with 85% remaining voltage, existing CF-Prev function, Inverter.

In Fig. 6.7, it can be seen that the inverter direct current rapidly increased to about

2 p.u. It then dropped to 0 p.u. at about 150ms. Consequently, the DC power also dropped to zero. The inverter rectifier angle also dropped to zero further signifying that successful commutation has failed to occur.

Fig. 6.8 shows that the delta group valve voltage collapsed to zero indicating that the commutation failure occurred in this valve group. The inverter zero sequence voltage is zero throughout the fault duration. This is expected since a symmetrical three phase to ground fault has been applied. It then becomes non-zero after the fault has been cleared due to the voltage imbalance that exists immediately after the fault is cleared.

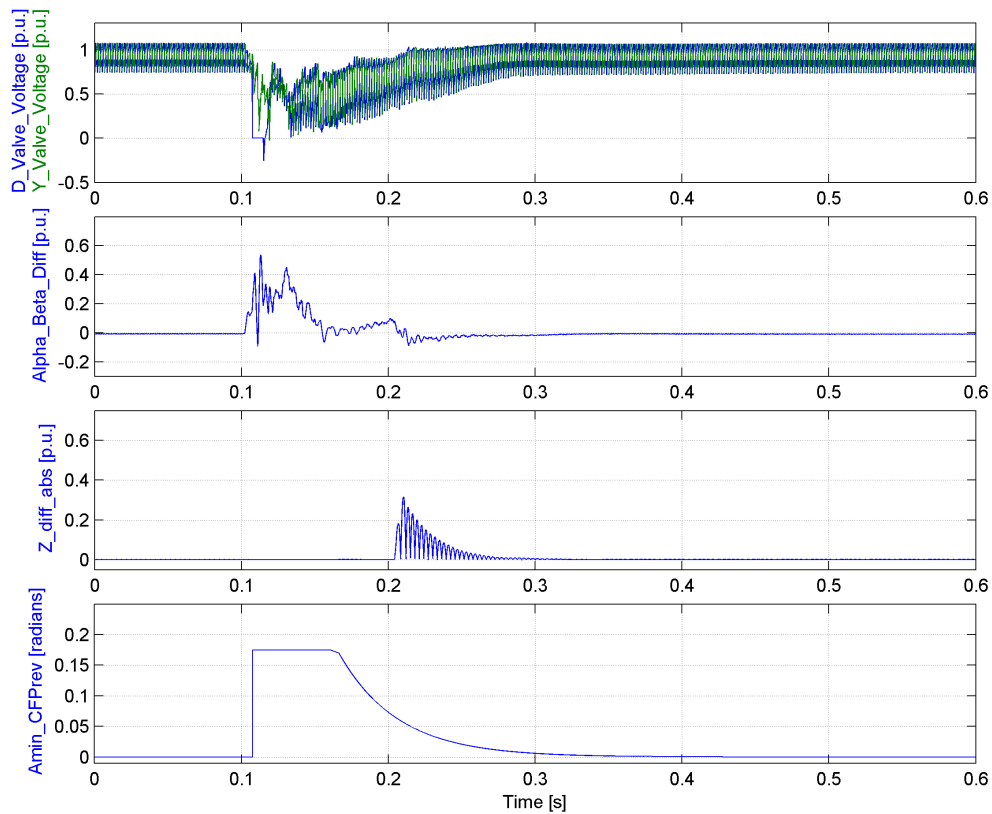


Figure 6.8: Three phase to ground fault with 85% remaining voltage, existing CF-Prev function, Inverter.

Moreover, it is evident that the CFPprev function activated and provided an output. However, it was unable to prevent the commutation failure. The system was able to recover and return to steady state at about 320ms.

Proposed CFPREV Function

The same fault as described in section 6.1.1.2 was applied however, in this case the proposed CFPREV function was utilised. The obtained results are presented in Fig. 6.9. The direct current increased to slightly above 2 p.u. then dropped to 0 p.u. The overlap angle also decreased to zero indicating the occurrence of a commutation failure.

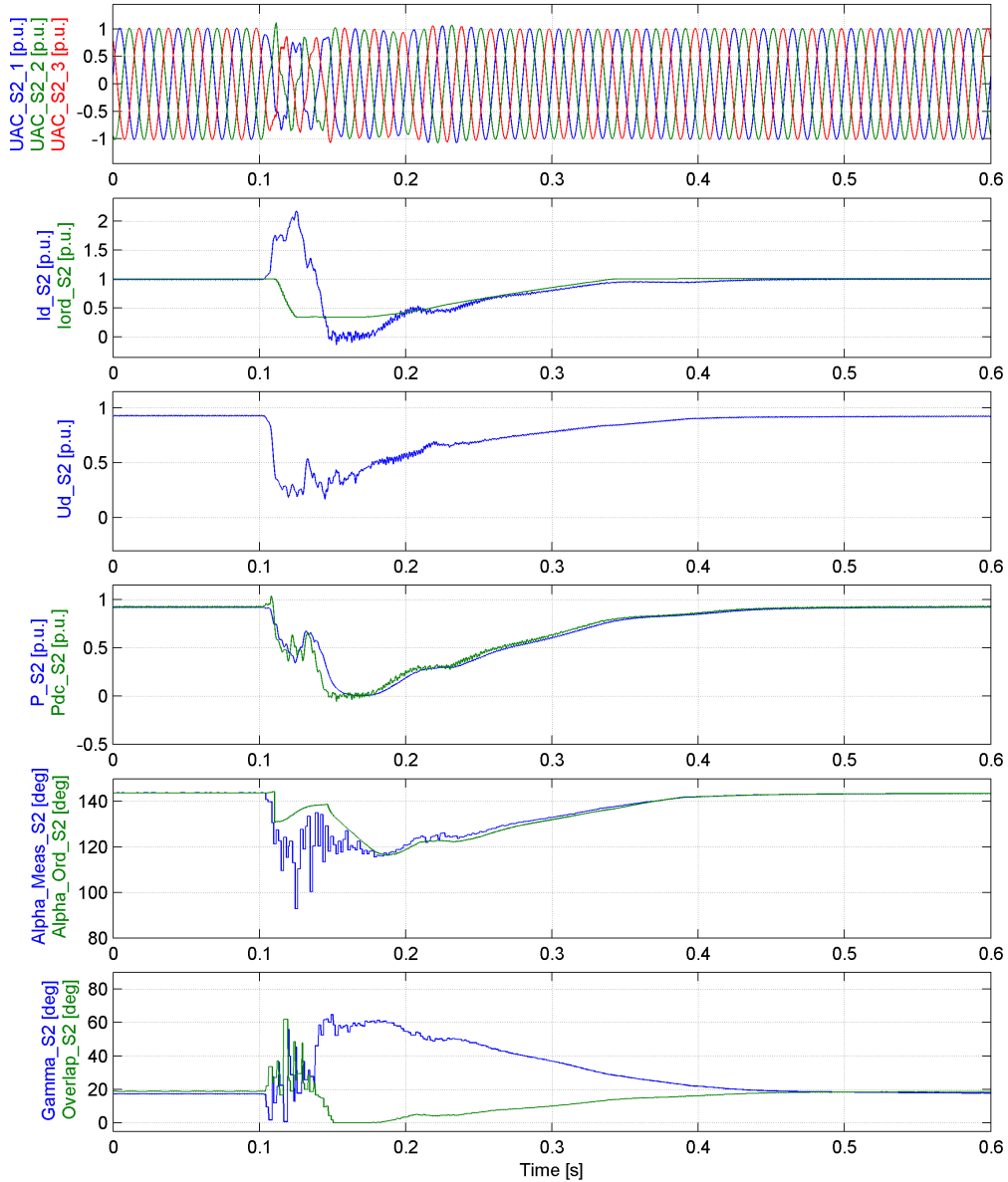


Figure 6.9: Three phase to ground fault with 85% remaining voltage, proposed CFPREV function, Inverter.

Fig. 6.10 shows that the delta group valve voltage collapsed to zero indicating that the commutation failure occurred in this valve group. The proposed CFPrev is activated twice, initially its activated when the Alpha_Beta_Diff value exceeded the preset threshold. Then it was also activated when the Z_diff value exceeded its preset threshold.

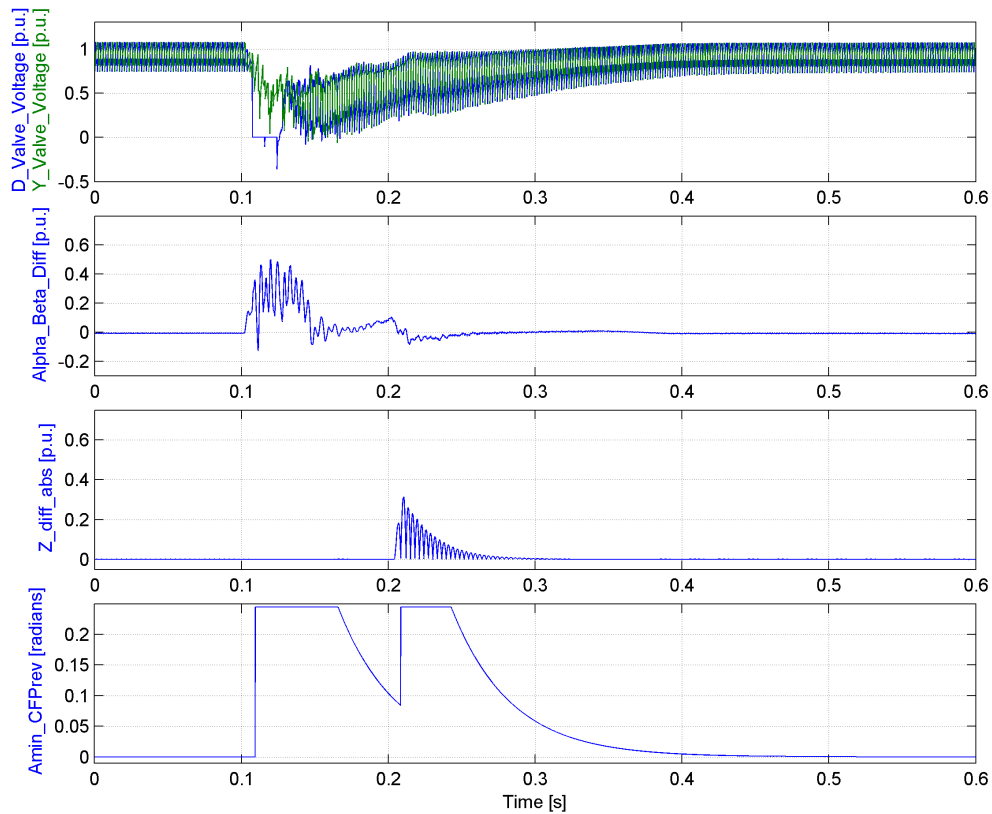


Figure 6.10: Three phase to ground fault with 85% remaining voltage, proposed CFPrev function, Inverter.

Despite being activated twice, the Proposed CFPrev is not able to guarantee successful commutation. The system recovered and returned to steady state at about 400ms.

6.1.2 Weak Network

The results presented under this section were obtained from simulations where both the rectifier and inverter AC grids were tuned to have SCRs of 3.

6.1.2.1 Single phase to ground faults

Existing CFPprev Function

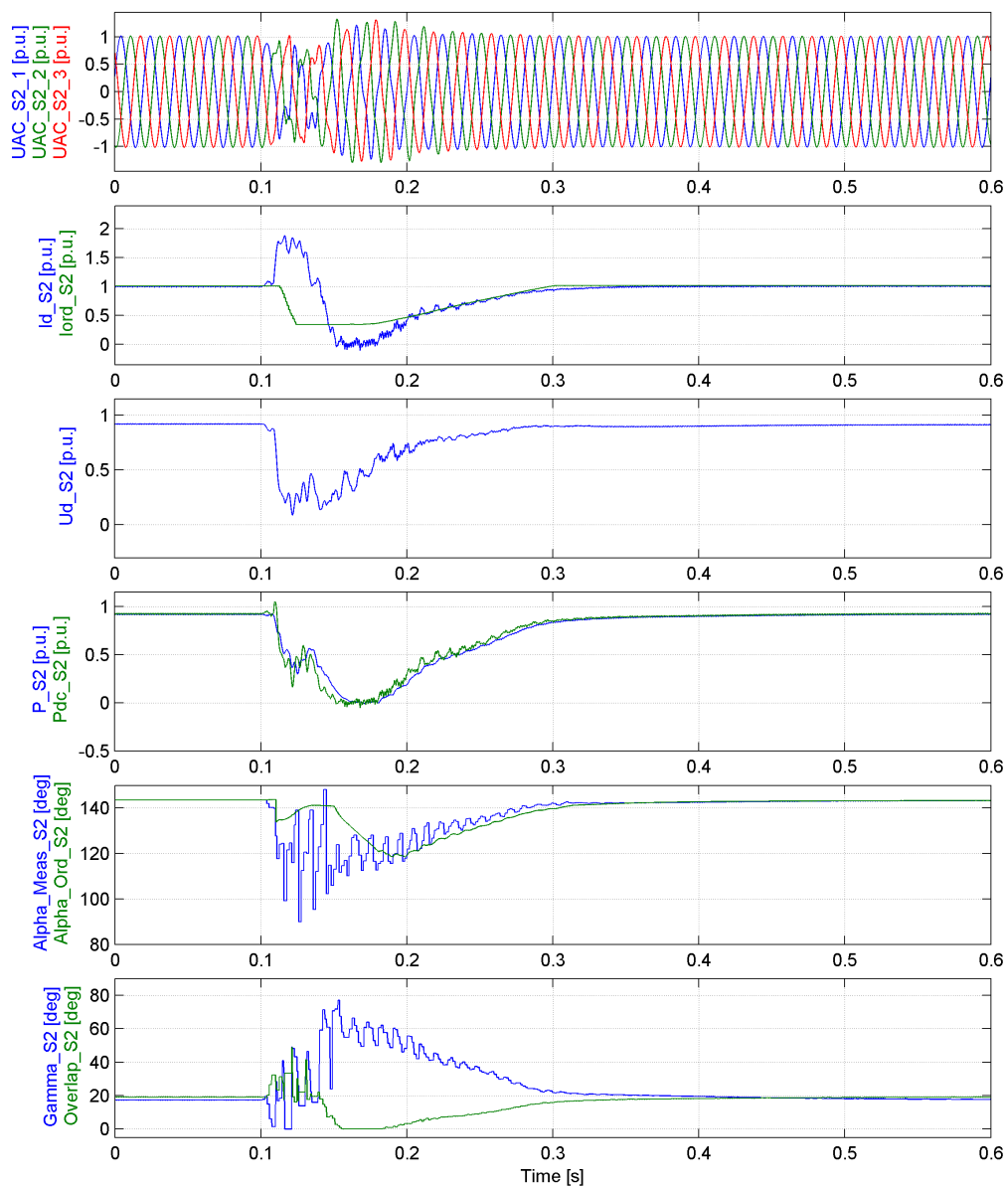


Figure 6.11: Single phase to ground fault with 87% remaining voltage, existing CFPprev function, Inverter.

6. Results and Discussions

A single phase to ground fault with a remaining voltage of about 87% was applied on the inverter side. The obtained results are presented in Fig. 6.11. It can be seen that commutation failure occurred since the overlap angle dropped to zero.

Fig. 6.12, shows that wye group valve voltage collapsed to zero indicating that the failed commutation occurred in this valve group. The CFPrev function activated but was not able to prevent commutation failure.

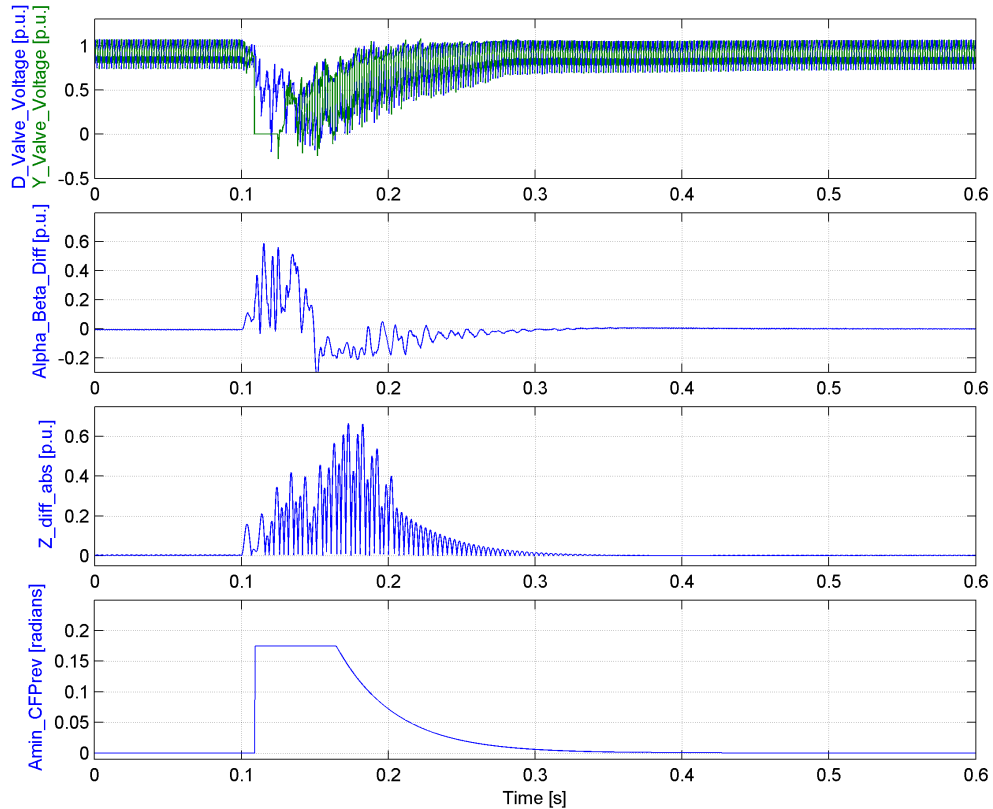


Figure 6.12: Single phase to ground fault with 87% remaining voltage, existing CFPrev function, Inverter.

Proposed CFPrev Function

When a single phase to ground fault with a remaining voltage of about 87% was applied, no commutation failure was observed. Fig. 6.13, shows that the direct current slowly increased to about 1.3 p.u., then it later dropped to about 0.7 p.u. before returning to 1 p.u. at about 350ms. The DC voltage dropped to about 0.75 p.u. as a result of the fault, it later recovered and returned to 1 p.u.

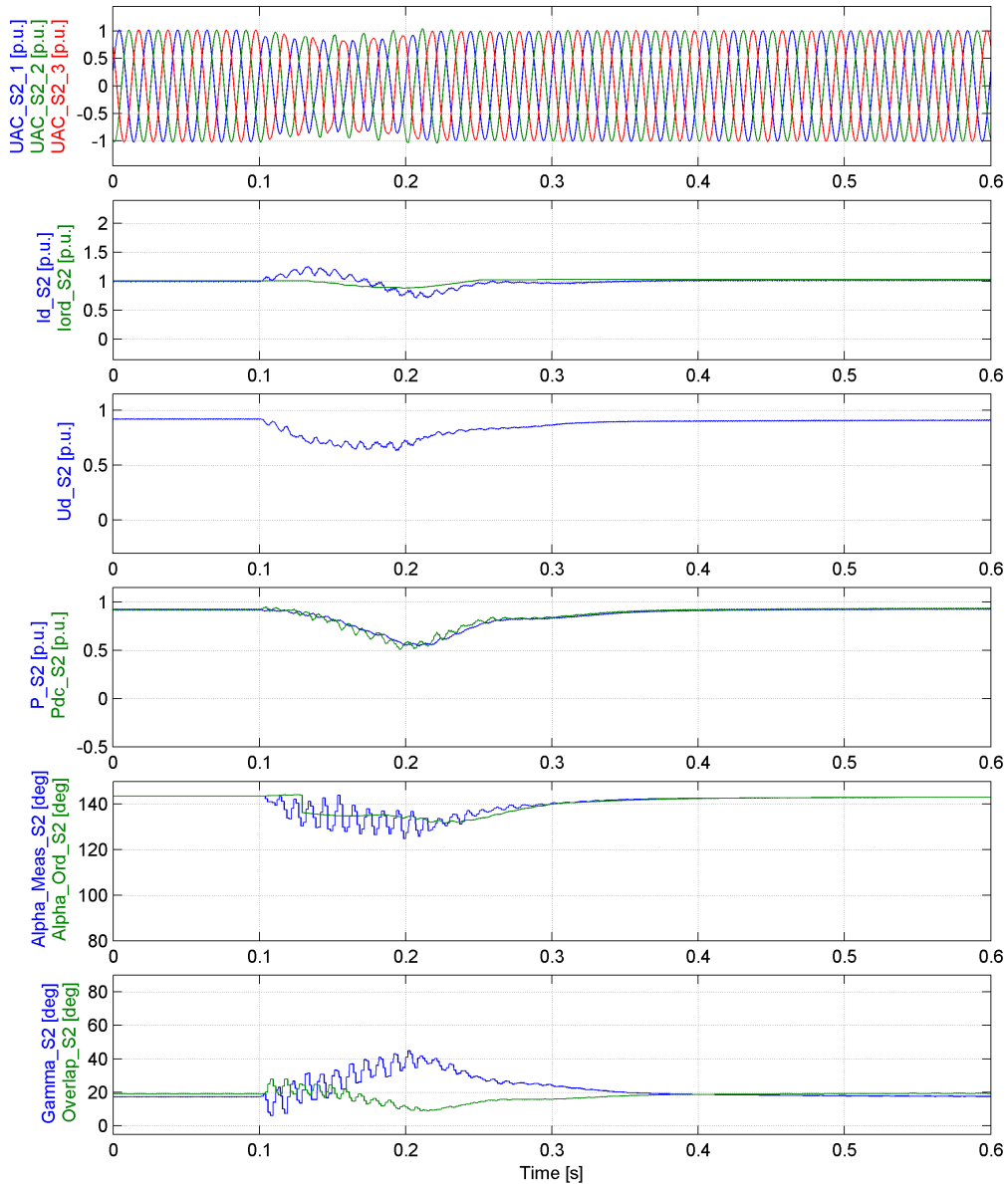


Figure 6.13: Single phase to ground fault with 87% remaining voltage, proposed CFPrev function, Inverter.

The extinction angle was slightly increased, this can be attributed to the actions of

the CFPrev function. The overlap angle dropped but it did not drop to reach zero.

Fig. 6.14 shows the proposed CFPrev function was activated and it was in position to facilitate successful commutation.

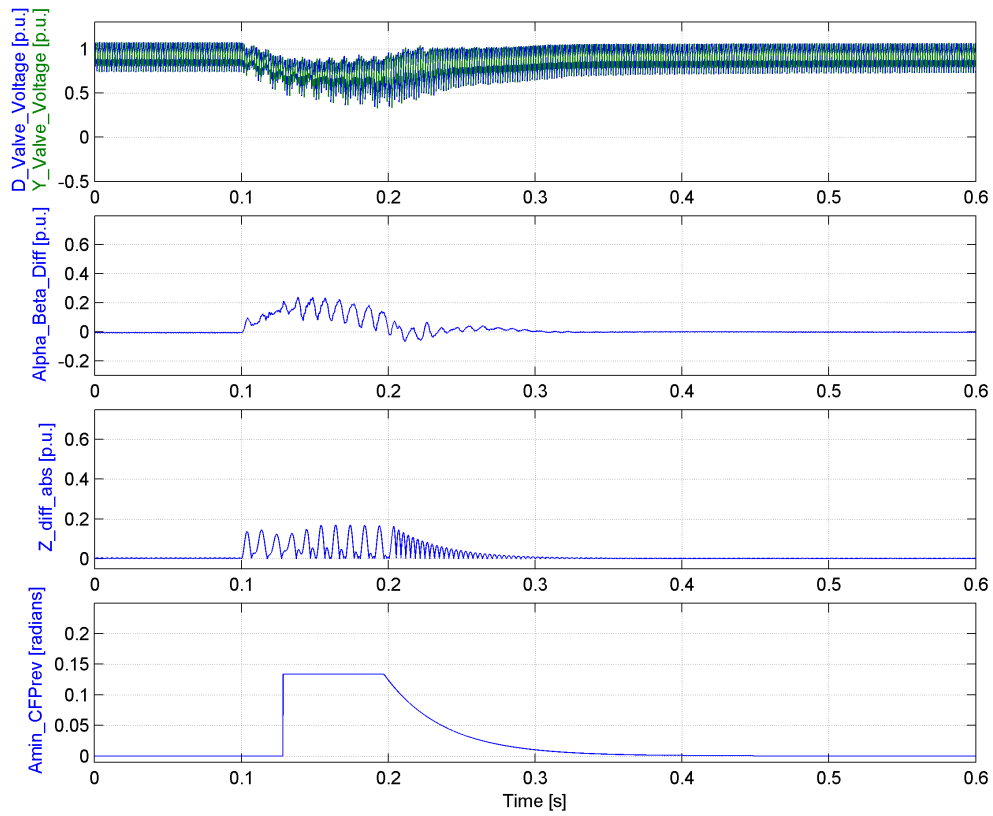


Figure 6.14: Single phase to ground fault with 87% remaining voltage, proposed CFPrev function, Inverter.

6.1.2.2 Three phase to ground faults

Existing CFPrev Function

When a three phase to ground fault with a remaining voltage of about 90% was applied to the inverter AC network, commutation failure was observed. In this case, the fault was initiated at 102ms and applied for 100ms with the existing CFPrev utilised. The simulation results are shown in Fig. 6.15 and Fig. 6.16.

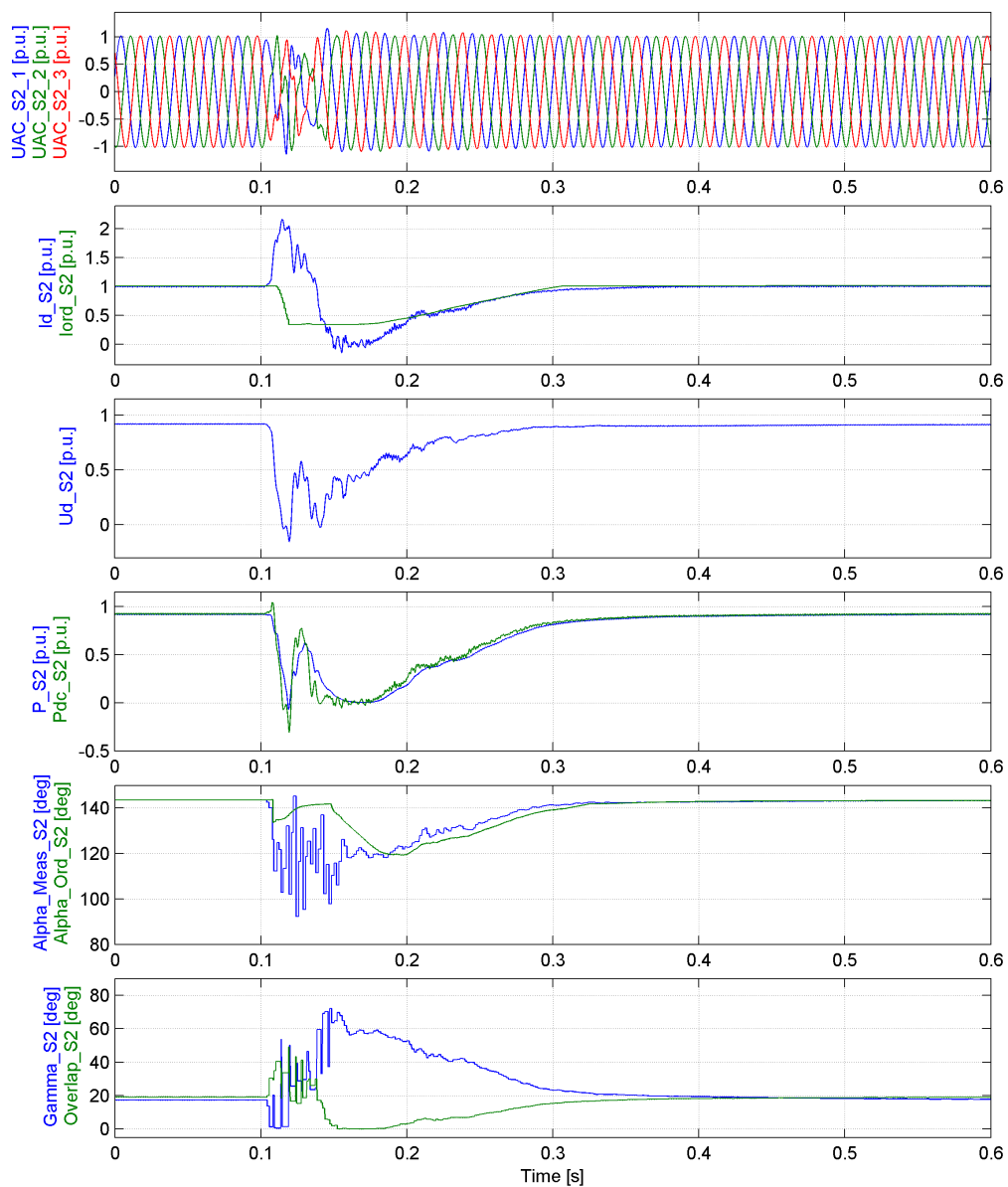


Figure 6.15: Three phase to ground fault with 90% remaining voltage, existing CFPrev function, Inverter.

6. Results and Discussions

The direct current rapidly increased to above 2 p.u. then dropped to 0 p.u. The DC power as well as the overlap angle also collapsed to 0 p.u.

In Fig. 6.16, it can be seen that both the delta and wye valve group voltages collapsed to 0 p.u. The occurrence of commutation failure in the delta valve group may have led to the failed commutation in the wye valve group.

Much as the CFPrev function was activated, it was unable to prevent commutation failures in any of the valve groups. The system was able to recover and return to steady state operation after the fault was cleared.

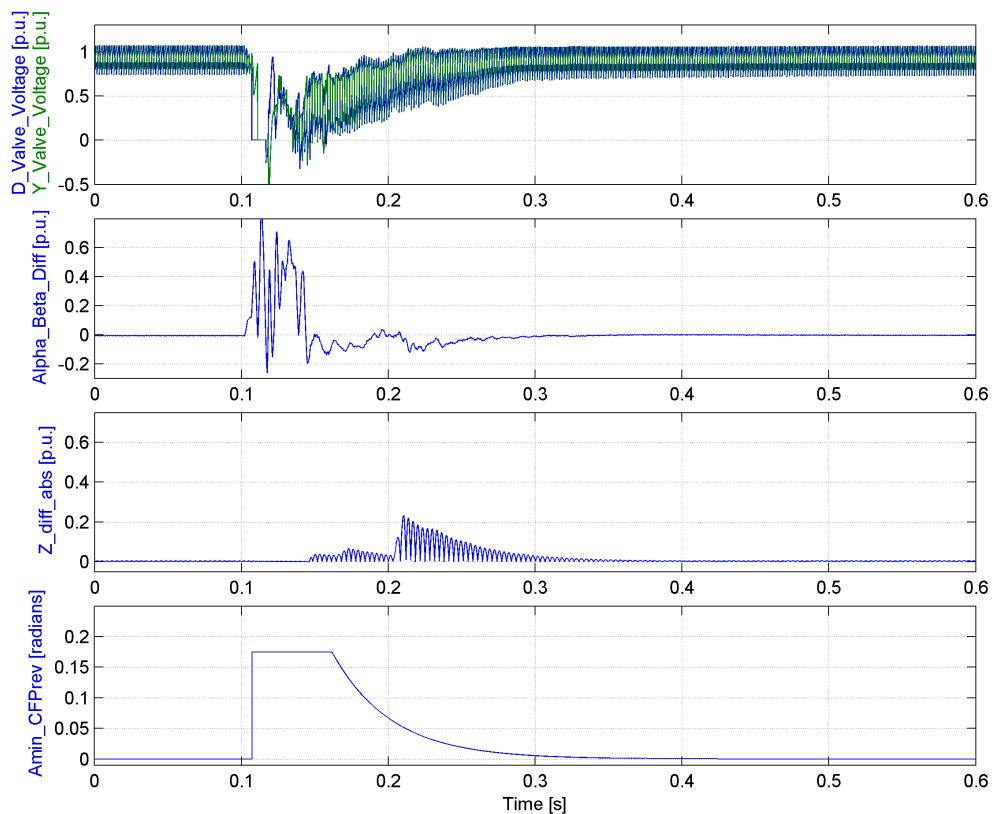


Figure 6.16: Three phase to ground fault with 90% remaining voltage, existing CFPrev function, Inverter.

Proposed CFPprev Function

When the same three phase to ground fault was applied but with the proposed CFPprev activated, no failed commutation was observed. The simulation results are shown in Fig. 6.17 and Fig. 6.18. The direct current slowly rises to about 1.4 p.u. then drops to about 0.6 p.u. it eventually rises to and stabilises at 1 p.u. The DC voltage decreases to approximately 0.6 p.u. while the DC power drops to 0.5 p.u.

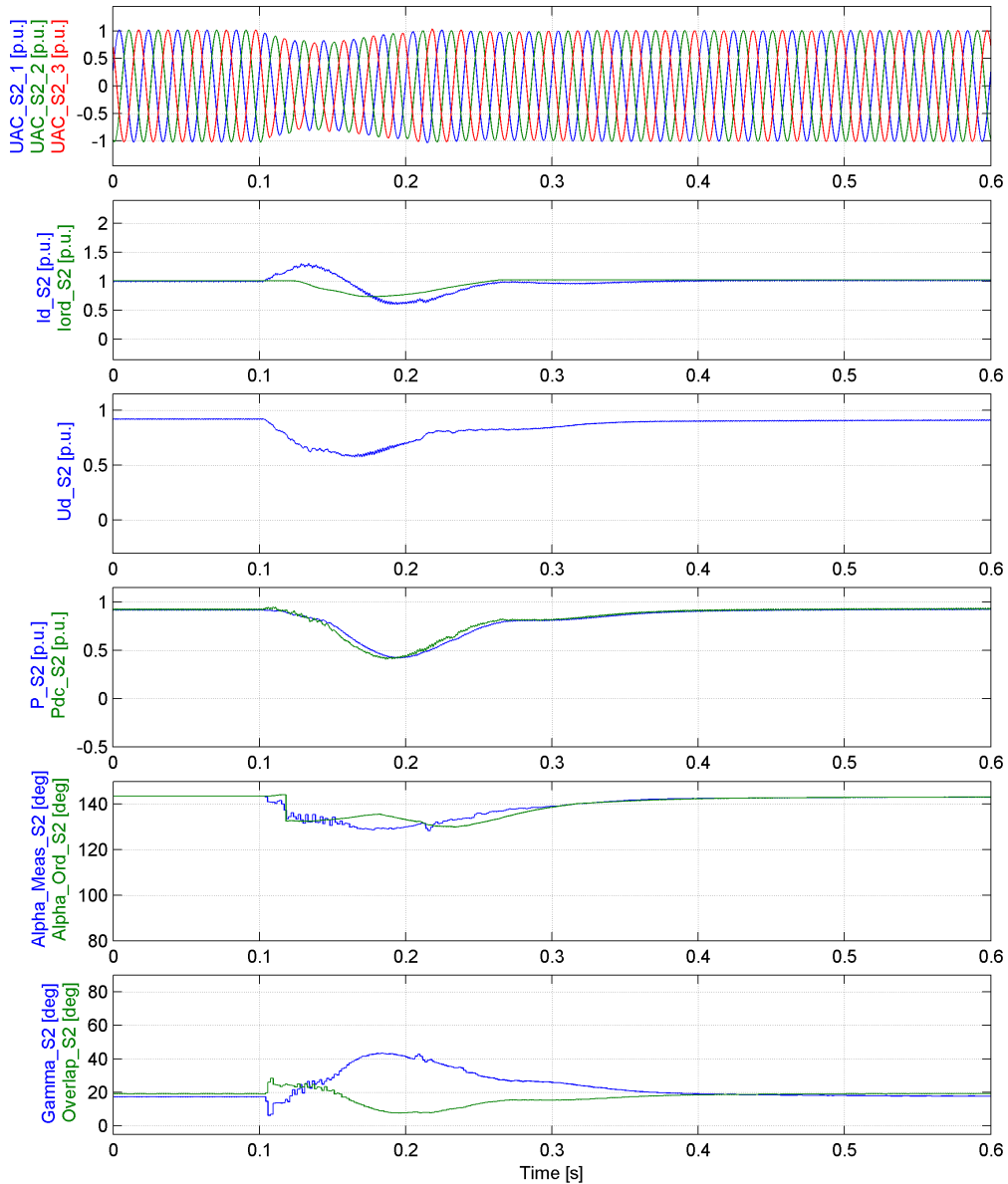


Figure 6.17: Three phase to ground fault with 90% remaining voltage, proposed CFPprev function, Inverter.

The overlap angle drops to about 10 degrees then slowly rises to approximately 20

degrees as the system recovers.

Fig. 6.18 shows no valve voltage collapse to 0 p.u. in either of the valve groups. The Proposed CFPrev function was activated and it was in position to prevent failed commutation.

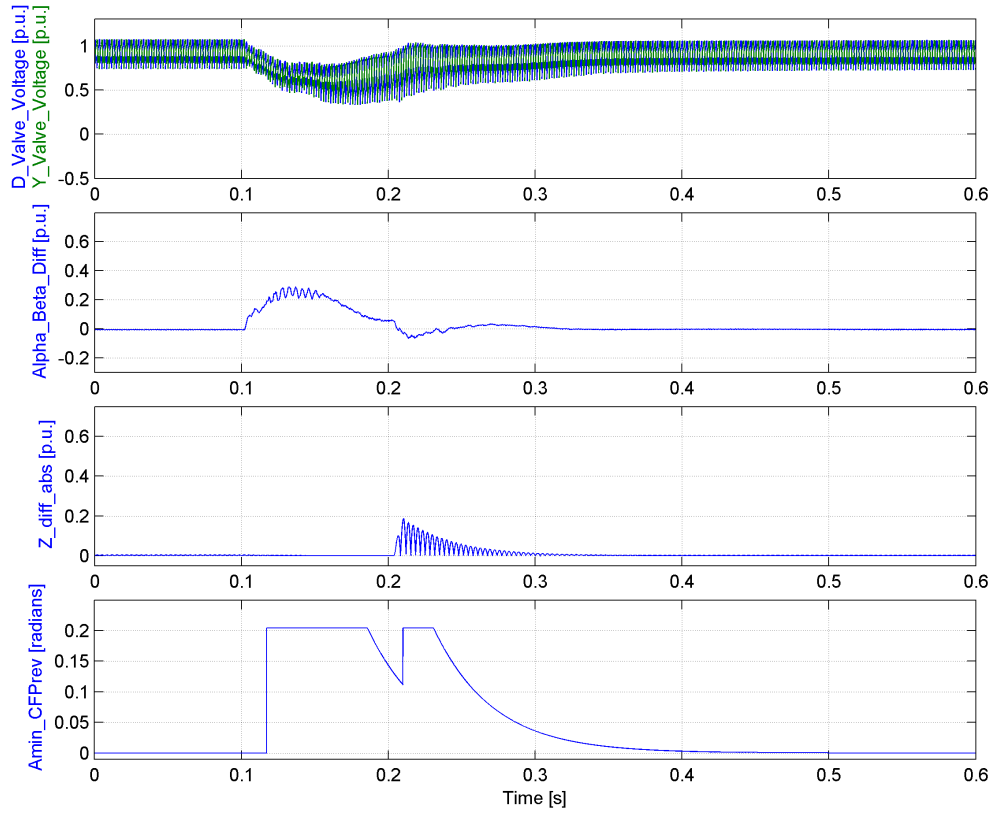


Figure 6.18: Three phase to ground fault with 90% remaining voltage, proposed CFPrev function, Inverter.

6.2 Point of wave scan

Due to the sinusoidal nature of the AC voltages, it was of interest to study the performance of the proposed CFP_{rev} function in relation to the fault initiation time. Simulations were carried for different fault initiations times, that is to say, the faults were initiated at different points along the AC voltage sine wave. Ten fault initiation times ranged from 100ms to 118ms (covering one complete cycle) with a time step of 2ms.

6.2.1 Strong Network

6.2.1.1 Single phase to ground faults

Single phase to ground faults with remaining voltages on the faulted phase ranging from 85% to 80% were applied to the inverter AC network with a SCR of 5 (strong network). The simulation results obtained were analysed and tabulated in Table. 6.2.

The yellow cells represent simulation cases where no failed commutation was observed. The green cells represent simulation cases where failed commutation occurred when the existing CFP_{rev} was activated but no failed commutation occurred with the proposed CFP_{rev}. The red cells signify the occurrence of commutation failure while both the existing and proposed CFP_{rev} functions are activated. The green cells show the improvements made in commutation failure prevention during single phase to ground faults when the proposed CFP_{rev} is utilised.

Table 6.2: Improvements in commutation failure prevention during single phase faults, strong network.

Remaining Voltage [%]	Fault Initiation Time [ms]										
	100	102	104	106	108	110	112	114	116	118	
85	Green	Yellow	Red	Yellow	Yellow	Yellow	Green	Red	Green	Yellow	
84	Green	Green	Red	Red	Red	Green	Red	Red	Red	Green	
83	Green	Green	Red	Red	Red	Green	Red	Red	Red	Red	
82	Green	Red	Red	Red	Red	Green	Red	Red	Red	Red	
81	Red	Red	Red	Red	Red	Red	Red	Red	Red	Red	
80	Red	Red	Red	Red	Red	Red	Red	Red	Red	Red	
	Yellow	No commutation failure									
	Green	Commutation failure with existing CFP _{rev}									
	Red	Commutation failure with both existing and proposed CFP _{rev}									

As can be seen in Table. 6.2, improvements are realised when the proposed CFP_{rev} is

utilised. For time instants such as 100ms, 102ms, 110ms, 112ms, 116ms and 118ms, the inverter valves experience no failed commutation when the proposed CFPrev is used as opposed to the existing CFPrev. This is so because the drop in voltage magnitude occurs before the start of commutation and the proposed CFPrev is able to sufficiently increase the extinction angle.

However, for 104ms, 106ms, 108ms and 114ms the proposed CFPrev function returns no improvements compared to the existing CFPrev. Both functions are unable to prevent failed commutation. This was because the drop in voltage occurred after the commutation on the next valve in the firing sequence had already begun. In such cases the CFPrev cannot prevent failed commutation.

6.2.1.2 Three phase to ground faults

Three phase to ground faults with remaining voltages on all the three phases ranging from 92% to 83% were applied to the inverter AC network with a SCR of 5. The simulation results obtained were analysed and tabulated in Table. 6.3.

It can be seen that no improvements are realised when the proposed CFPrev function is used as opposed to the existing CFPrev function. When a three phase to ground fault is applied, all the voltages are affected. Due to this, the chances of having a voltage drop after the commutation in the next valve in the firing sequence has started are largely increased.

Table 6.3: Improvements in commutation failure prevention during three phase faults, strong network.

Remaining Voltage [%]	Fault Initiation Time [ms]										
	100	102	104	106	108	110	112	114	116	118	
92	Yellow	Yellow	Red	Red	Yellow	Yellow	Yellow	Red	Red	Yellow	
90	Red	Red	Red	Red	Red	Red	Red	Red	Red	Red	
88	Red	Red	Red	Red	Red	Red	Red	Red	Red	Red	
86	Red	Red	Red	Red	Red	Red	Red	Red	Red	Red	
85	Red	Red	Red	Red	Red	Red	Red	Red	Red	Red	
83	Red	Red	Red	Red	Red	Red	Red	Red	Red	Red	
	Yellow	No commutation failure									
	Green	Commutation failure with existing CFPrev									
	Red	Commutation failure with both existing and proposed CFPrev									

Multi-valve failures

Since the proposed CFP_{rev} did not yield any improvements when three phase to ground faults were applied, its performance is investigated further with regard to multi-valve commutation failures. If for a given fault case, failed commutation occurred in more than one valve, this was considered as a multi-valve commutation failure. The results from this analysis are tabulated in Table. 6.4.

The yellow cells represent fault cases where no multi-valve commutation failures occurred. The red cells represent fault cases where multi-valve commutation failures occurred despite of the activation of both the existing and the proposed CFP_{rev} functions. The green cells represent fault cases where multi-valve commutation failures occurred when the existing CFP_{rev} was utilised but no multi-valve failed commutation was observed with the activation of the proposed CFP_{rev} function.

Table 6.4: Improvements in multi-valve commutation failure prevention during three phase faults, strong network.

Remaining Voltage [%]	Fault Initiation Time [ms]									
	100	102	104	106	108	110	112	114	116	118
92	Yellow	Yellow	Green	Green	Yellow	Yellow	Yellow	Green	Green	Yellow
90	Green	Green	Green	Green	Green	Green	Green	Green	Red	Green
88	Green	Green	Green	Green	Red	Green	Green	Red	Red	Red
86	Red	Green	Red	Red	Red	Red	Red	Red	Red	Red
85	Red	Green	Red	Red	Red	Red	Red	Red	Red	Red
83	Red	Red	Red	Red	Red	Red	Red	Red	Red	Red
	No multi-valve commutation failure									
	Multi-valve commutation failure with existing CFP _{rev}									
	Multi-valve commutation failure with existing and proposed CFP _{rev}									

From Table. 6.4, it is clear that the proposed CFP_{rev} is quite effective in reducing the occurrence of multi-valve commutation failures. When the proposed CFP_{rev} is activated, multi-valve commutation failures generally start to occur when the remaining voltage is approximately 88%. However, when the existing CFP_{rev} is activated, multi-valve commutation failures start to occur with a remaining voltage of about 92%.

6.2.2 Weak Network

6.2.2.1 Single phase to ground faults

Single phase to ground faults with remaining voltages on the faulted phase ranging from 90% to 81% were applied to the inverter AC network with a SCR of 3 (weak network). The simulation results obtained were analysed and tabulated in Table. 6.5. The green cells represent fault cases where improvements were observed with the proposed CFPprev activated. Improvements were observed only for certain time instances such as 100ms, 106ms and 116ms.

Notice that for the 100ms with a remaining voltage of 85%, a failed commutation occurred irrespective of the activation of both the existing and proposed CFPprev functions. For a similar fault case in Table. 6.2, no failed commutation was observed. This is attributable to the different SCRs of the AC networks.

Table 6.5: Improvements in commutation failure prevention during single phase faults, weak network.

Remaining Voltage [%]	Fault Initiation Time [ms]									
	100	102	104	106	108	110	112	114	116	118
90	Yellow	Yellow	Yellow	Yellow	Yellow	Yellow	Yellow	Yellow	Yellow	Yellow
89	Green	Red	Yellow	Yellow	Yellow	Yellow	Red	Yellow	Yellow	Yellow
87	Green	Red	Red	Green	Yellow	Yellow	Red	Red	Green	Yellow
85	Red	Red	Red	Green	Red	Red	Red	Red	Green	Red
83	Red	Red	Red	Green	Red	Red	Red	Red	Green	Red
81	Red	Red	Red	Red	Red	Red	Red	Red	Red	Red
Yellow	No commutation failure									
Green	Commutation failure with existing CFPprev									
Red	Commutation failure with both existing and proposed CFPprev									

Table. 6.5 also shows that when the remaining voltage drops to about 81% of the pre-fault voltage, commutation failures cannot be avoided even with the proposed CFPprev function. With a weak network, the improvements attained from the use of the proposed CFPprev function are fewer compared to those with a strong network (see Table. 6.2).

6.2.2.2 Three phase to ground faults

Three phase to ground faults with remaining voltages on all the three phases ranging from 92% to 83% were applied to the inverter AC network with a SCR of 3 (weak network). The simulation results obtained were analysed and tabulated in Table. 6.6.

It can be seen that only one improvement (when the fault is initiated at 102ms with a remaining voltage of 90%) was realised when the proposed CFPprev function is used as opposed to the existing CFPprev function. The performance of the proposed CFPprev is quite similar to that shown in Table. 6.3.

Table 6.6: Improvements in commutation failure prevention during three phase faults, weak network.

Remaining Voltage [%]	Fault Initiation Time [ms]										
	100	102	104	106	108	110	112	114	116	118	
92	Red	Yellow	Yellow	Red	Red	Red	Yellow	Yellow	Red	Red	
90	Red	Green	Red	Red	Red	Red	Red	Red	Red	Red	
88	Red	Red	Red	Red	Red	Red	Red	Red	Red	Red	
86	Red	Red	Red	Red	Red	Red	Red	Red	Red	Red	
85	Red	Red	Red	Red	Red	Red	Red	Red	Red	Red	
83	Red	Red	Red	Red	Red	Red	Red	Red	Red	Red	
	Yellow	No commutation failure									
	Green	Commutation failure with existing CFPprev									
	Red	Commutation failure with both existing and proposed CFPprev									

Multi-valve failures

The results from the analysis of multi-valve commutation failures are shown in Table. 6.7. It is important to note that, the improvements in commutation failure prevention are lower compared to the results obtained for the strong network in Table. 6.4.

Table 6.7: Improvements in multi-valve commutation failure prevention during three phase faults, weak network.

Remaining Voltage [%]	Fault Initiation Time [ms]										
	100	102	104	106	108	110	112	114	116	118	
92	Green	Yellow	Yellow	Green	Green	Red	Yellow	Yellow	Green	Green	
90	Red	Green	Green	Red	Red	Red	Green	Red	Red	Red	
88	Red	Red	Green	Red	Red	Red	Red	Red	Red	Red	
86	Red	Red	Red	Red	Red	Red	Red	Red	Red	Red	
85	Red	Red	Red	Red	Red	Red	Red	Red	Red	Red	
83	Red	Red	Red	Red	Red	Red	Red	Red	Red	Red	
	Yellow	No multi-valve commutation failure									
	Green	Multi-valve commutation failure with existing CFPprev									
	Red	Multi-valve commutation failure with existing and proposed CFPprev									

6.3 Comparison of different SCRs

For this section the value of Amin-ref-gain was varied from 0 to 2 for different SCRs. This was done to investigate the relationship between the Amin-ref-gain value required to prevent commutation failure and the SCR. Single phase to ground faults with a remaining voltage of approximately 82% of the pre-fault voltage were applied to the inverter AC network.

Both the rectifier and inverter AC network SCRs were varied from 3, 4, 5, 7 and 10. When the network SCR was 10 no failed commutation occurred however, with a SCR of 3 commutation failure prevention was not possible. At each SCR, a different minimum value of Amin-ref-gain was required to prevent the occurrence of failed commutation.

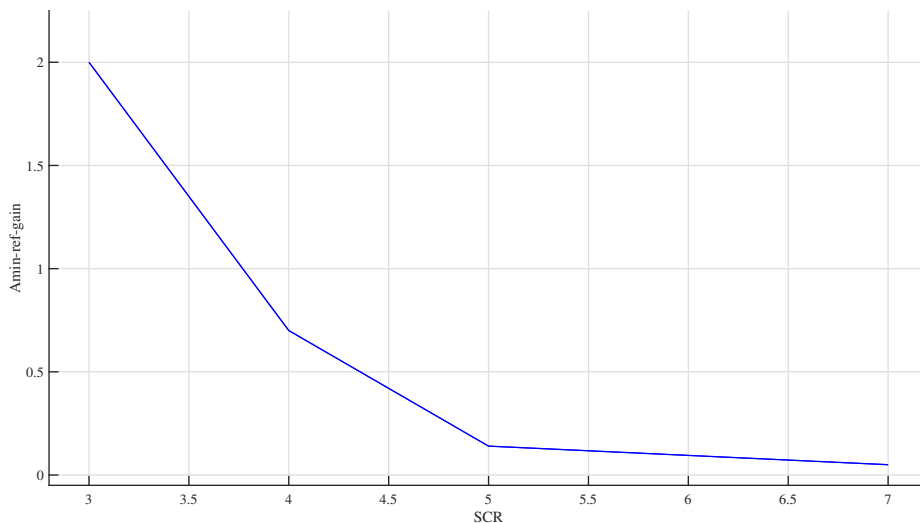


Figure 6.19: Relationship between Amin-ref-gain and SCR

It was discovered that the stronger networks required a smaller value of Amin-ref-gain to prevent the occurrence of commutation failure compared to the weak network.

7

Conclusions

The main aim of designing and implementing a CFPrev function based on a Voltage time area contribution has been achieved. The new CFPrev function was designed by introducing subtle changes to the existing CFPrev function. It has been shown through simulations that the proposed CFPrev functions has advantages over the existing function.

The proposed function was effective in mitigating the first commutation failure when single phase faults with remaining voltages ranging from 85% to 82% were applied to the strong inverter AC grid. However, less success was registered when the single phase to ground faults were applied to weak inverter AC grids. This can be attributed to the large increase in the inverter's reactive power consumption when the inverter extinction angle is increased.

Furthermore, when three phase to ground faults with remaining voltages ranging from 92% to 83% were applied to strong inverter AC grids, the proposed CFPrev function was unable to mitigate the commutation failures. Its actions were rather similar to those of the existing CFPrev. This was because the functions increased the extinction angle while the commutation of current had already started. This chain of events rendered both CFPrev functions ineffective. When the same three phase to ground faults were applied to weak inverter AC grids, the proposed CFPrev function was able to mitigate at least one commutation failure.

Since the proposed CFPrev was limited in mitigating the initial commutation failures after the initiation of three phase faults, further investigations with regard to multi-valve commutation failure were carried out. The proposed CFPrev greatly reduced the occurrence of multi-valve failed commutation with both strong and weak inverter AC grids.

The functionality of the proposed CFPrev was checked for different AC grid SCRs. It was discovered that the stronger the AC grid was, the more likely the function was to mitigate commutation failures. While applying single phase to ground faults with a remaining voltage of 82%, The Amin-ref-gain of the function was varied from 0 to 2 for different SCRs. It was noted that AC grids with SCRs greater than or equal to 5 required Amin-ref-gain of 0.25 or less to mitigate the first commutation failure. The weaker AC grids required Amin-ref-gain greater than 1.4.

When Amin-ref-gain is increased beyond 2, the CFPprev function becomes disadvantageous to the HVDC system. These results are presented in Appendix 1. It leads to further commutation failures instead of mitigating them. It also affects the recovery of the system after the fault has been successfully cleared.

Commutation failures begin to occur when the AC voltage of weak grids is reduced by 8% - 10%. This is because the low SCR of the weak inverter AC grid increases the commutation reactance on the inverter side, resulting in a larger overlap angle. Consequently, lowering the extinction angle of the inverter. This makes the inverter valves more prone to commutation failures.

In conclusion, the simulation results show that the proposed CFPprev function is 17% more effective in mitigating commutation failures when single phase faults were applied in comparison to the existing function. Furthermore, the results show that in 25% of the simulated cases when three phase faults were initiated, the proposed function reduced the occurrence of multi-valve failures. Moreover, proper tuning of the Amin-ref-gain is essential to ensure that the activation proposed function does not lead to commutation failures and poor system recovery.

7.1 Future Work

The performance of the proposed CFPprev function when single phase and three phase faults occurred was investigated. However, the effects of AC voltage phase shift and rapid increase of direct current were not studied. These two could present an interesting area to evaluate in future work.

The effect of having a cable within the HVDC transmission link instead of only an overhead link presents another opportunity for future work. Furthermore, the effectiveness of the proposed function in mitigating commutation failures for different inverter extinction angles can also be studied.

Bibliography

- [1] Z. Wei, Y. Yuan, X. Lei, H. Wang, G. Sun, and Y. Sun, "Direct-current predictive control strategy for inhibiting commutation failure in hvdc converter," *Power Systems, IEEE Transactions on*, vol. 29, no. 5, pp. 2409–2417, 2014.
- [2] L. Zhang and L. Dofnas, "A novel method to mitigate commutation failures in hvdc systems," in *Power System Technology, 2002. Proceedings. PowerCon 2002. International Conference on*, vol. 1. IEEE, 2002, pp. 51–56.
- [3] E. Rahimi, A. Gole, J. Davies, I. T. Fernando, and K. Kent, "Commutation failure analysis in multi-infeed hvdc systems," *Power Delivery, IEEE Transactions on*, vol. 26, no. 1, pp. 378–384, 2011.
- [4] Y.-Z. Sun, L. Peng, F. Ma, G. Li, and P. Lv, "Design a fuzzy controller to minimize the effect of hvdc commutation failure on power system," *Power Systems, IEEE Transactions on*, vol. 23, no. 1, pp. 100–107, 2008.
- [5] R. Rudervall, J. Charpentier, and R. Sharma, "High voltage direct current (hvdc) transmission systems technology review paper," *Energy week*, vol. 2000, p. 2, 2000.
- [6] C.-K. Kim, V. K. Sood, G.-S. Jang, S.-J. Lim, and S.-J. Lee, *HVDC transmission: power conversion applications in power systems*. John Wiley & Sons, 2009.
- [7] C. Barker, "Hvdc for beginners and beyond," 2009.
- [8] Å. Ekström, *High power electronics HVDC and SVC*. Royal Institute of Technology, 1990.
- [9] Cigre, "Commutation failures—causes and consequences," *Cigre Working Group 14.05, Paris*, 1995.
- [10] F. Jansson, "Converter firing control for classic hvdc," *ABB 1JNL100108-929 Rev.01*, 2006.
- [11] "Hvdc control," *ABB 1JNL100020-842 Rev.00*.

- [12] K. Lindén, “Overview of the hvdc control system,” *ABB 1JNL100033-106 Rev.01*, 2001.
- [13] Å. Ekström and G. Liss, “A refined hvdc control system,” *Power Apparatus and Systems, IEEE Transactions on*, no. 5, pp. 723–732, 1970.
- [14] E. W. Kimbark, *Direct current transmission*. John Wiley & Sons, 1971, vol. 1.
- [15] A. Muthusamy, “Selection of dynamic performance control parameters for classic hvdc in pss/e,” 2010.
- [16] C. Thio, J. Davies, K. Kent, and G. Andersson, “Commutation failures in hvdc transmission systems. discussion,” *IEEE Transactions on Power Delivery*, vol. 11, no. 2, pp. 946–957, 1996.
- [17] “Dynamic performance study,” *ABB power systems LF 2197 Ludvika*, 1992.

A

Appendix 1

Single phase to ground fault with a remaining voltage of 85%

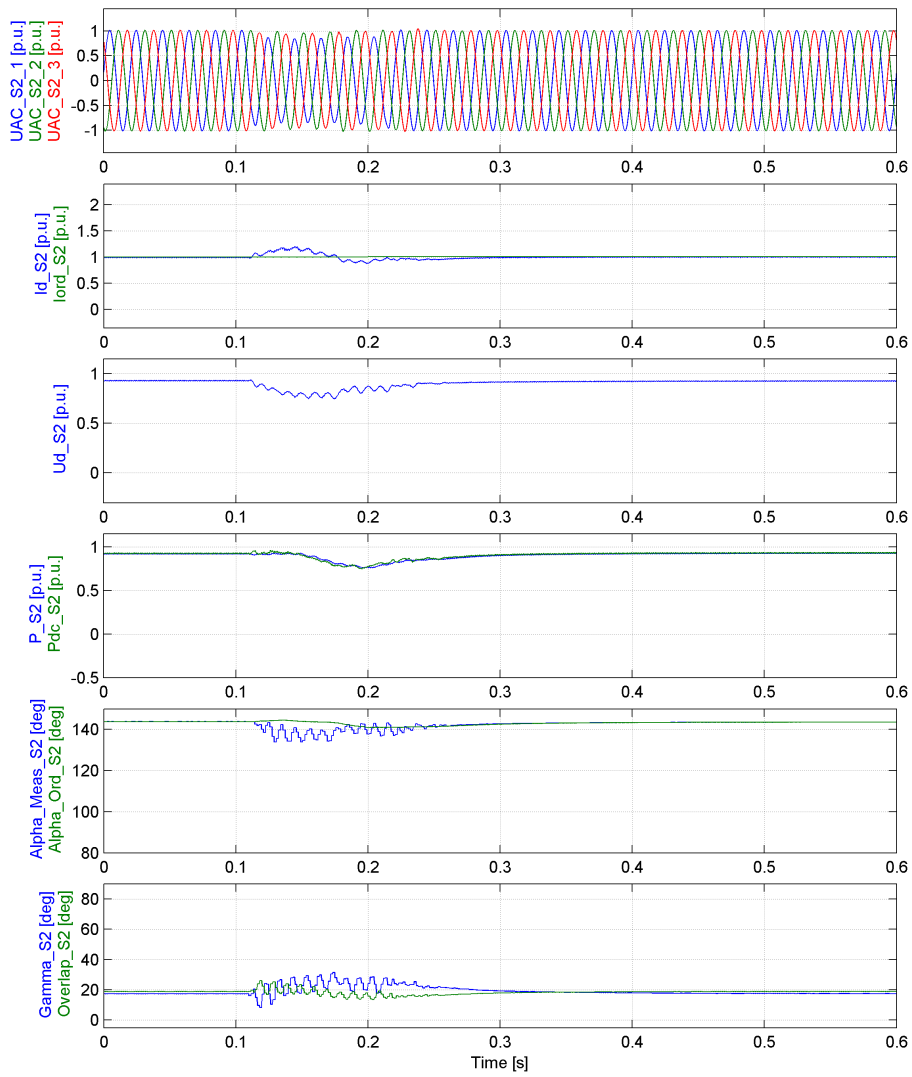


Figure A.1: Existing CFPprev function, inverter.

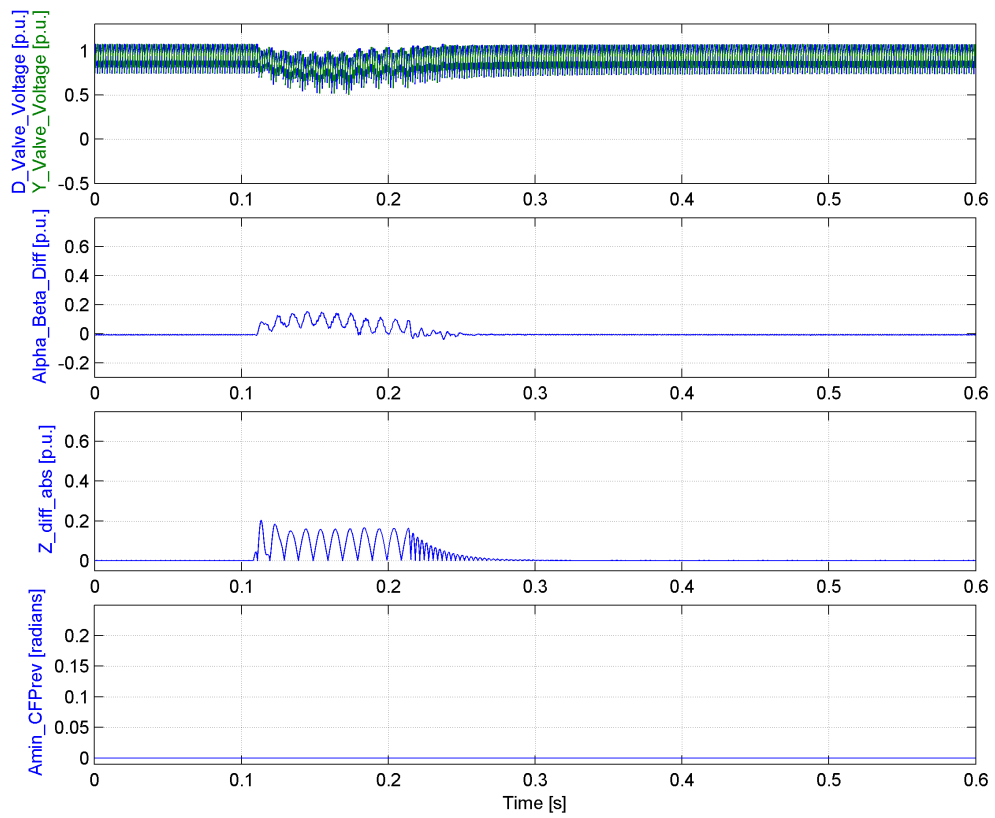


Figure A.2: Existing CFFPrev function, Inverter.

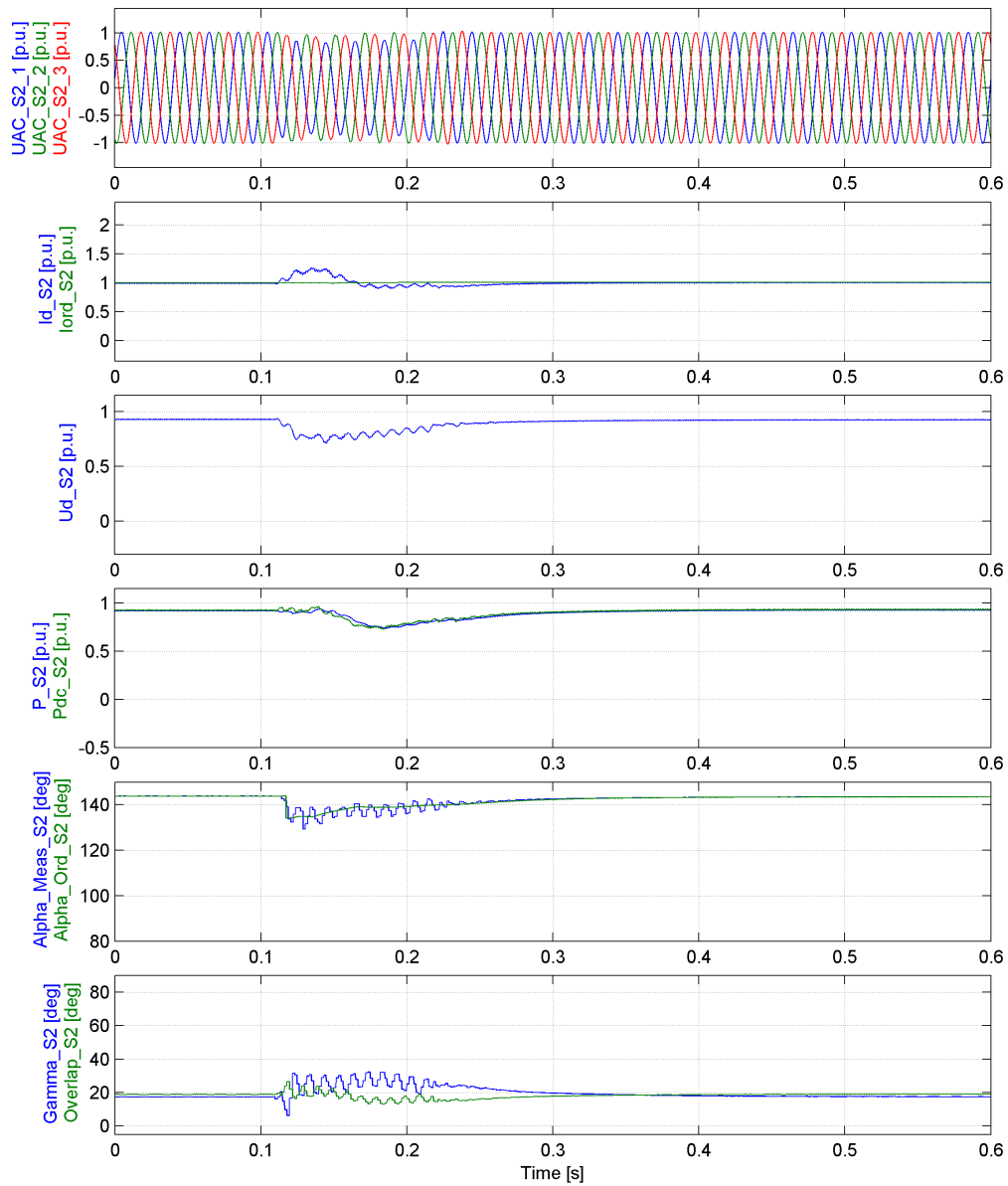


Figure A.3: Proposed CFPprev function, Amin-ref-gain = 0.5, Inverter.

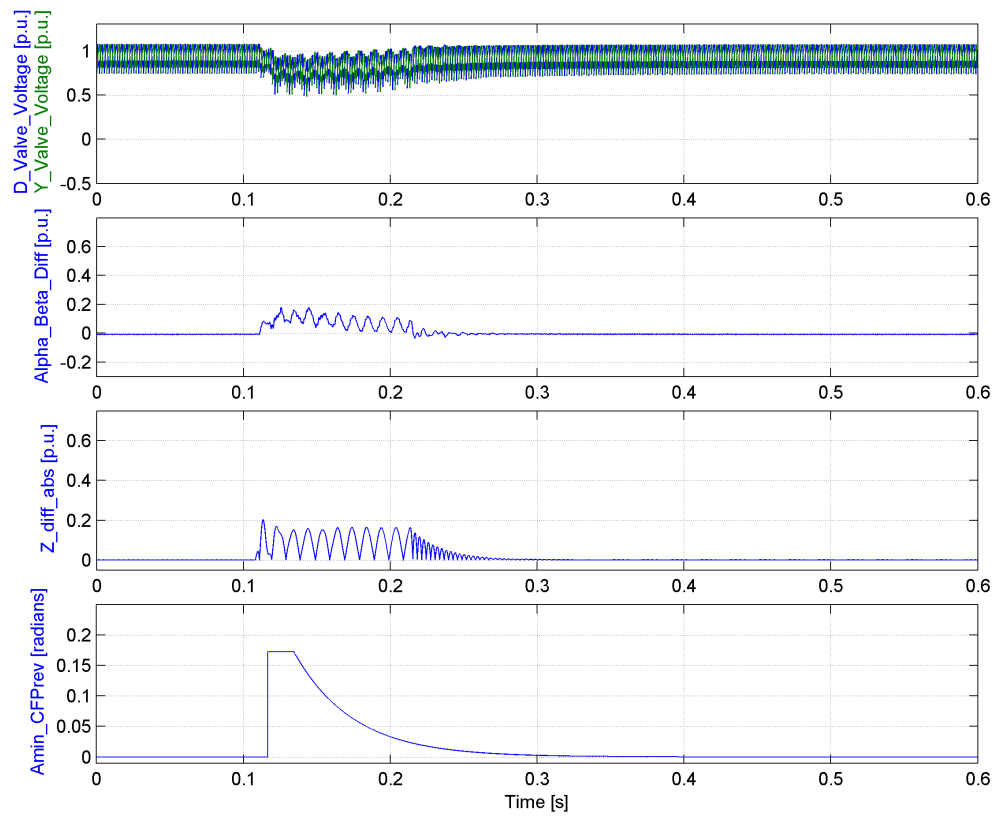
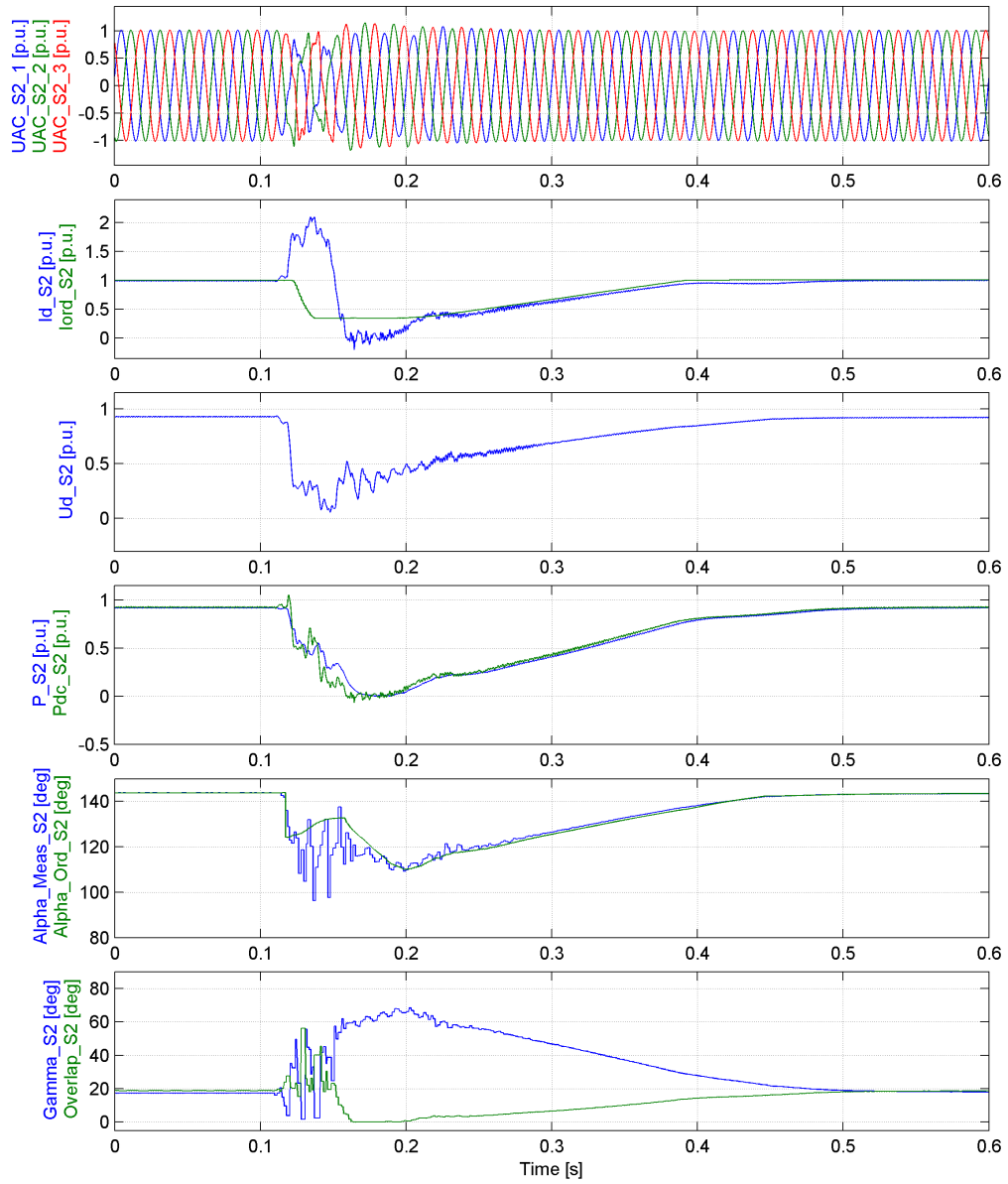


Figure A.4: Proposed CFPprev function, Amin-ref-gain = 0.5, Inverter.

Figure A.5: Proposed CFPrev function, $A_{min-ref-gain} = 2$, Inverter.

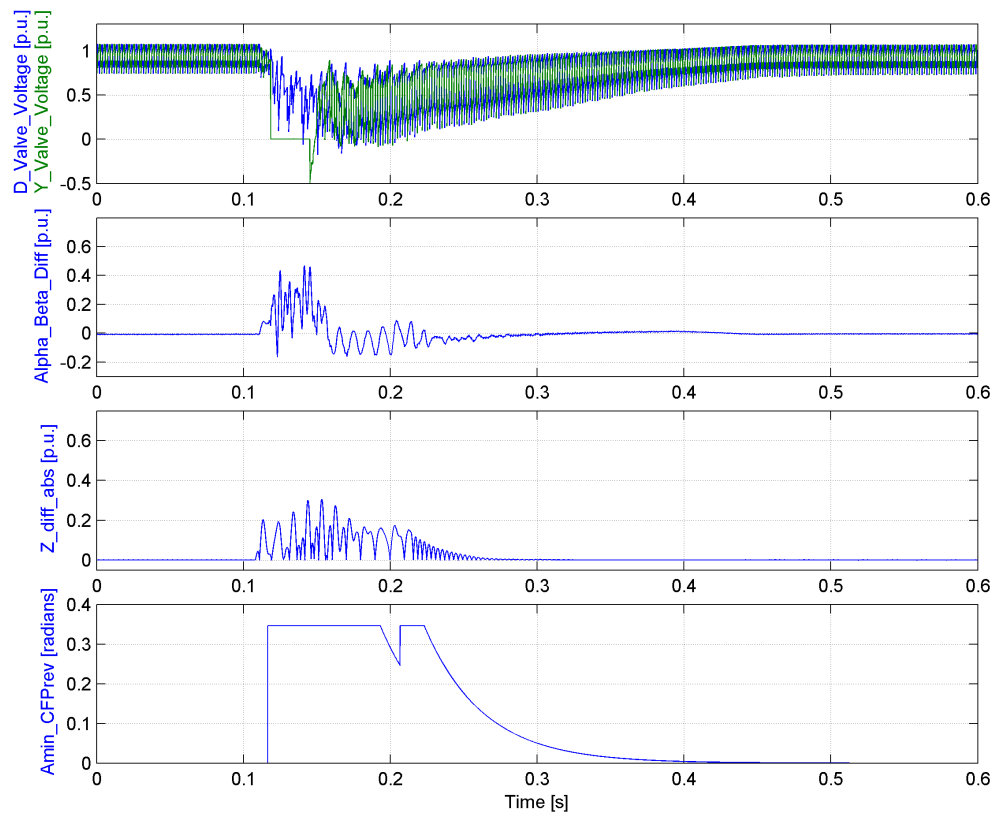


Figure A.6: Proposed CFPprev function, Amin-ref-gain = 2, Inverter.